PREPARED FOR THE U.S. DEPARTMENT OF ENERGY,
UNDER CONTRACT DE-AC02-76-CHO-3073

PPPL-2908
UC-421,422,427

PPPL-2908

THEORY OF CONTINUUM DAMPING OF TOROIDAL ALFVÉN EIGENMODES IN FINITE-β TOKAMAKS

BY

F. ZONCA AND L. CHEN

MAY, 1993

PRINCETON
PLASMA PHYSICS
LABORATORY

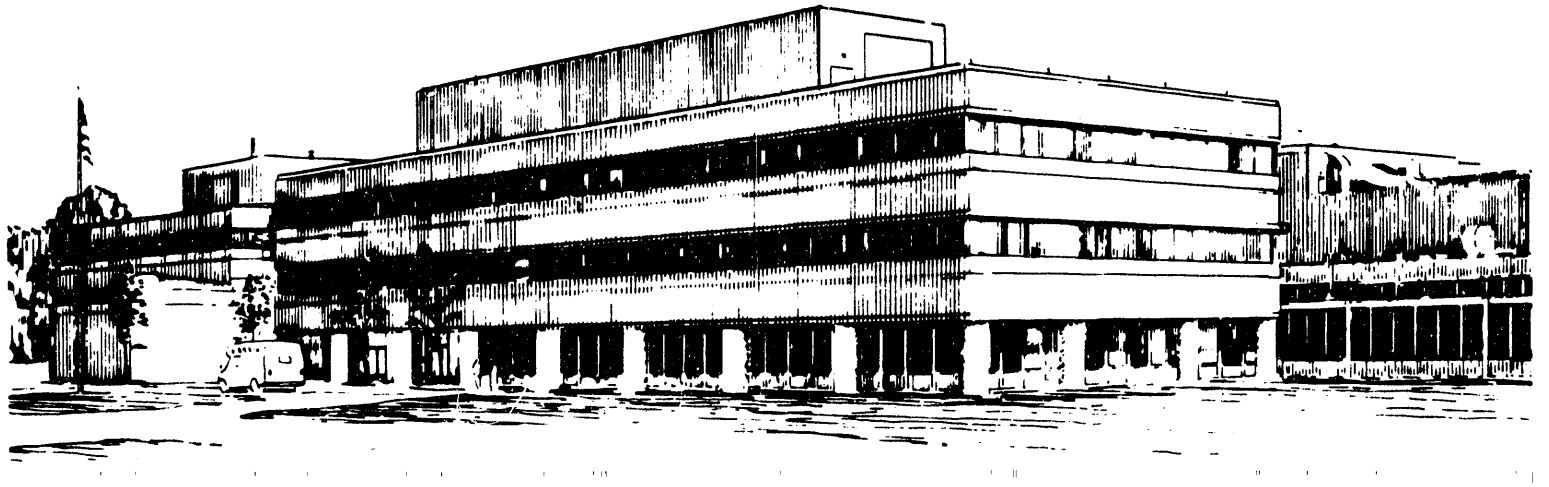

NOTICE

April 7, 1993

Theory of Continuum Damping of Toroidal Alfvén Eigenmodes in finite-β Tokamaks

Fulvio Zonca*and Liu Chen

Plasma Physics Laboratory and

Department of Astrophysical Sciences

Princeton University, Princeton, NJ 08543

Abstract

We have formulated a general theoretical approach for analyzing two-dimensional structures of high-n Toroidal Alfvén Eigenmodes (TAE) in large aspect-ratio, finite-β tokamaks. Here, n is the toroidal wave number and β is the ratio between plasma and magnetic pressures. The present approach generalizes the

*Permanent Address: Associazione EURATOM-ENEA sulla Fusione, C.P. 65-00044 Frascati, Rome, ITALY.

standard ballooning-mode formalism and is capable of treating eigenmodes with extended global radial structures as well as finite coupling between discrete and continuous spectra. Employing the well-known (s, α) model equilibrium and assuming a linear equilibrium profile, we have applied the present approach and calculated the corresponding resonant continuum damping rate of TAE modes. Here, s and α denote, respectively, the strengths of magnetic shear and pressure gradients. In particular, it is found that there exists a critical α value, $\alpha_c(s)$, such that, as $\alpha \rightarrow \alpha_c$, the continuum damping rate is significantly enhanced and, thus, could suppress the potential TAE instability.

PACS numbers: 52.35.Bj; 52.55.Dy; 52.55.Fa

I. Introduction

The confinement properties of energetic particles in fusion plasmas are of major importance in determining the performance of current and future generations of machines operating near or at reactor relevant regimes. For example, the good confinement of alpha particles produced in the DT fusion reactions is necessary to ignite the DT plasma. Similarly, energetic ions produced in RF or neutral beam injection experiments must be well confined in order to successfully achieve plasma heating and/or current drive. While the theoretically predicted confinement properties of energetic particles based on Coulomb collisions are sufficiently adequate, there remain serious concerns over "anomalous" losses induced by collective oscillations spontaneously excited by the energetic particles.

Since the fusion alphas are born at $3.52MeV$ mainly in the plasma center, the corresponding pressure profile is peaked. As a consequence, the energetic-particle pressure gradient is a free energy source that can destabilize waves which resonantly interact with the periodic motion of the energetic particles.[1-3] As typically in the case of pressure-gradient driven modes, the instability growth rates increase with the energetic-particle diamagnetic drift frequency which is proportional to the toroidal mode number n. On the other hand, characteristic frequencies of the energetic-particle motion (e.g., transit and bounce) are estimated to be in the Mhz range; similar to that of shear Alfvén waves. This observations thus suggest that high-n ($n >> 1$) shear Alfvén waves are the prime candidate for the instabilities.

Shear Alfvén waves in a laboratory plasma are, however, difficult to excite, since energy is needed to bend the magnetic field lines. Moreover, in a sheared magnetic field, the shear Alfvén waves are characterized by a continuous spectrum.[4] Thus,

these waves are highly localized around the surface where $\omega = k_{||} v_A$ (ω is the mode frequency, $k_{||}$ is the wave vector parallel to the magnetic field and $v_A = B/\sqrt{4\pi\varrho}$ the Alfvén speed, ϱ being the plasma mass density), and strongly stabilized because of phase mixing.

This situation, strictly valid in a slab, is qualitatively modified in toroidal confinement devices due to the poloidal symmetry breaking associated with toroidal magnetic field inhomogeneities over a magnetic surface. The resultant couplings between neighbouring poloidal harmonics produces not only frequency gaps[5] in the continuous shear Alfvén spectrum, but also discrete Alfvén eigenmodes.

These discrete modes, known as TAE (Toroidal Alfvén Eigenmodes[6,7]), are localized in the forbidden frequency window ('gap') of the shear Alfvén (shear Alfvén) continuum. As a consequence, TAE's are undamped, to the lowest order, due to their negligible coupling to the continuum.

That TAE's are marginally stable naturally suggests that energetic particles can resonantly destabilize these modes. Furthermore, these resonant energetic particles could also be effectively scattered by the resultant Alfvénic fluctuations. Indeed, it has been shown that even low-amplitude TAE's, with $\delta B/B \approx 5\text{x}10^{-4}$, can cause severe fusion alpha particles losses.[8] The study of the linear stability of TAE's is, therefore, an important issue for tokamak fusion research, and has attracted increasing theoretical as well as experimental interest.[9,10]

The linear TAE drive, due to the resonant interaction of the mode with the periodic transit of the passing energetic particles has been extensively studied.[11-14] The weakening effect on the linear drive because of resonance detuning due to finite particle drift orbits has also been considered.[15] Recently,[16,17] it has been pointed

out that both passing and trapped particles play important roles in determining the linear drive.

A number of damping mechanisms have been suggested by various authors to balance the energetic-particle linear drive and, hence, to determine the marginal stability threshold for TAE's. Electron Landau damping[11–14] is typically negligible, while ion Landau damping[14] and trapped electron collisional damping[18,19] could be important depending on the plasma parameters.[17] Another effective damping mechanism, due to the coupling of the TAE mode to the continuous shear Alfvén spectrum, was suggested first in Ref. [11] and studied in detail in Ref. [20] and Ref. [21] for the high-n case, and in Ref. [22] for low-n. In this case, the damping is a consequence of the toroidal mode coupling, which renders the TAE global radial mode width much broader than the typical radial extent of a single poloidal harmonic.[20] In the present paper, we would like to clarify the details of Ref. [20] and present important new results when a finite pressure is included in the employed model equilibrium.[23,24]

To delineate the mechanism of TAE's coupling to the shear Alfvén continuum, it is instructive to recall the nature of the continuous shear Alfvén spectrum in a screw pinch with periodic length $2\pi R_o$ and an equilibrium magnetic field $\vec{B} \equiv (0, B_\theta(r), B_z(r))$. Here, (r, θ, z) refer to cylindrical coordinates. In this case, shear Alfvén waves consist of *local* oscillations with frequency

$$\omega^2(r) \;=\; k_{\|}^2(r)\, v_A^2(r) \;=\; \frac{(nq(r)-m)^2}{q^2(r)R_o^2}\, v_A^2(r) \qquad (1)$$

varying throughout the plasma column. Here, $q(r) = rB_z(r)/R_oB_\theta(r)$ plays the role of the safety factor in a tokamak, and we have assumed the following dependence:

$$\delta\phi(r,\theta,z,t) \;=\; e^{i(nz/R_o - m\theta)}\delta\phi_{m,n}(r,t)\;, \qquad (2)$$

for the scalar potential perturbation $\delta\phi$. Thus, shear Alfvén waves are characterized by $\delta\phi_{m,n}(r,t) \approx a(r,t)\exp(-i\omega(r)t)$ with $\omega(r)$ given by Eq. (1), and $a(r,t)$, typically, decays time asymptotically as $1/t$ due to *phase mixing.*[4]

When the cylindrical equilibrium is bent into a torus, the variation of the Alfvén speed on a magnetic flux surface causes different poloidal harmonics to be coupled together. As a consequence,[5] the cylindrical continuous shear Alfvén spectra of the m and $m+1$ poloidal harmonics couple at $r = r_o$, where $k_{\|m+1,n} = -k_{\|m,n}$ or, equivalently, where $nq(r_o) - (m+1) = -(nq(r_o) - m)$ (i.e. $nq(r_o) - m = 1/2$), and a gap appears in the shear Alfvén continuum as shown in Fig.1. From Eq. (1), the local oscillation frequency of these coupled harmonics is close to $\omega_o^2 = v_A^2(r_o)/4q^2(r_o)R_o^2$, and the frequency gap width scales linearly with $\epsilon_o = O(a/R_o)$, the strength of the toroidal coupling. Here, a and R_o are, respectively, the minor and the major radii. The discrete mode (the TAE), meanwhile, exists inside the gap[6,7] and has a radially localized eigenfunction with a typical radial width ϵ_o/nq'. Note that, in the present analysis, $\epsilon_o < 1$, i.e., we have in mind tokamaks with large aspect ratios. The physical origin of the *local potential well* which allows TAE's to exist as discrete modes is discussed in detail in Ref. [24].

Due to toroidicity, each poloidal harmonic is coupled to its neighbour, as sketched in Fig.2. However, only a finite number of poloidal harmonics will be coupled to determine the global TAE radial structure. In fact, radial equilibrium changes will cause a mismatch in the oscillation frequencies of poloidal harmonics peaked in frequency gaps located at different radial positions. This frequency mismatch dictates that the local mode structure (and, hence, the local oscillation frequency) of the various poloidal harmonics must readjust in order to constructively

form a global plasma oscillation with a given frequency ω_{TAE}. This is obviously possible only for a limited number of harmonics, whose coupling gives rise to the global TAE width. The amplitudes of the poloidal harmonics outside this global TAE width decay exponentially fast; since they are no longer effectively excited (see Fig.3).

The excited frequency of the *global TAE mode* falls within the frequency gaps at different radial positions within a region $\epsilon_o L_A$, with L_A being the scale length of the Alfvén frequency $\omega_A = v_A/q(r)R_o$. Outside this region, harmonics of the shear Alfvén continuous spectrum are resonantly excited, but usually have a small amplitude (exponentially small) because of the frequency mismatch mentioned above. The resultant coupling of the TAE modes to the shear Alfvén continuum is, thus, also expected to be small; indicating, consequently, a small damping coefficient.

Figure 3 allows us to make some general remarks on TAE modes. First, the number of poloidal harmonics coupled to form the global TAE radial structure is $|\Delta m| \approx |n\Delta q| \approx n\epsilon_o|q'L_A|$. Thus, many harmonics are coupled together if $n\epsilon_o >> 1$; suggesting $n\epsilon_o$ is an important asymptotic parameter. Moreover, $|\Delta m/m| \approx |\Delta q/q| \approx \epsilon_o|q'L_A| << 1$, indicating that the spread Δm is small compared to the central mode number m_o if the toroidal coupling effects are weak. Second, the global TAE radial width $\Delta r_{TAE} \approx \epsilon_o L_A$ is small compared to the equilibrium scales, but still rather broad, since it does not decrease with n. Finally, the radial structure of the TAE mode (i.e., the *two-dimensional TAE structure*) is of crucial importance to determine its coupling to the continuous spectrum and, hence, its continuum damping. In particular, it is important to determine where the TAE is localized within the gap region, the distances from the accumulation points of the continua,

and how fast the *radial envelope* of the global mode decays away from the TAE localization region.

For pressureless equilibria with circular magnetic flux surfaces[20,21] it has been demonstrated that TAE modes are always well localized within the gap region. In the present work, we will show that finite pressure shifts the global TAE structure toward the accumulation point of the lower continuum; leading, thus, to greatly enhanced continuum damping rates. This may be expected from Fig.3, since the amplitudes of the poloidal harmonics resonantly excited in the continuum would be of the same order of those forming the global mode structure. The expected damping rate is then typically of $O(\epsilon_o \omega_A)$.

In Section II, the theoretical formulation for the two-dimensional TAE eigenmode analysis is presented. In general, this problem can be reduced to the solution of two nested one-dimensional ordinary differential equations: the first one solves for the mode structure along the field lines on a local flux surface. The second one correlates the local solutions and prescribes how, starting from them, the global two-dimensional eigenmode can be constructed. This procedure is conceptually similar to that of the well-known ballooning formalism,[25-27] but, as will be shown later, it has some important qualitative differences. Furthermore, it may be applied to the analysis of various high-n two-dimensional perturbations other than TAE modes.

In Section III, we will use the well known (s, α) model equilibrium[28,29] ($s = rq'/q$ is the magnetic shear and $\alpha \equiv -R_o q^2 \beta'$ is the normalized pressure gradient, $\beta \equiv$ plasma pressure/magnetic pressure) to derive the relevant equations for high-n TAE modes in axisymmetric tokamak equilibria with shifted circular magnetic

surfaces and $\beta = O(a/R_o)$. The motivation of this choice is that, for weakly shaped equilibria, such a model is sufficiently general and still simple enough to allow substantial analytical progress. However, it needs to be emphasized that similar analyses could also be carried out for general equilibria; except in such cases extensive numerical solutions will be required.

Since, for the practical purpose, the continuum damping rate is expected to be small compared to the frequency gap width $\epsilon_o\omega_A/2$, we will obtain its general analytic expression using a perturbative approach, which is naturally formulated as a variational principle. Hence, in Section IV, the two-dimensional TAE eigenmode structure is obtained, to the lowest order, neglecting the coupling to the shear Alfvén continuous spectrum.

The general expression for the Alfvén continuum damping rate is derived in Section V. To show in detail how the damping rate may be computed; in Section VI a model linear equilibrium profile is assumed to further reduce the continuum damping to a readily usable expression. The corresponding results are analyzed in Section VII. In particular, as discussed earlier, it is shown that, near the Troyon β-limit,[30] the TAE suffers a greatly enhanced damping.

Finally, Section VIII contains a summary and discussions. In order to present the physics more clearly, we have chosen to keep the mathematical details to a minimum in the main text. Detailed derivations can be found either in Ref. [24] or in the two Appendices, in which some relevant technical details are treated in depth.

II. Theoretical Formulation

In this Section, we present a systematic analysis of high-n two-dimensional eigenmode structures in axisymmetric toroidal equilibria. In developing this approach, we have been strongly motivated by the original works of Connor, Hastie and Taylor[25] as well as Dewar and coworkers,[26] who have developed complementary formalisms for the study of two-dimensional high-n ideal magnetohydrodynamic ballooning modes in tokamaks. All these analyses employ the WKB approximation along with $1/n$ expansions to reduce the starting two-dimensional equations to two nested one-dimensional problems. While our approach shares the same conceptual foundation with that of the previous papers,[25,26] there are, as it will be discussed later, important qualitative differences.

Let us consider the solution of the following high-n eigenmode equation

$$\mathcal{D}\left(\omega; r, \vartheta, \partial_r, \partial_{\vartheta}\right) \delta\phi(\omega; r, \vartheta) = 0 \ . \tag{3}$$

Here, we assume that $\mathcal{D}$ is a partial differential operator defined on a domain $\Sigma \in R^2$, and that the boundary conditions on $\delta\phi$ are such that

$$\int\int_{\Sigma} |\delta\phi(\omega; r, \vartheta)|^2 J(r, \vartheta) dr d\vartheta = \mathcal{E}(\omega) < \infty \ ; \tag{4}$$

where $J(r, \vartheta) = |\vec{\nabla} r \times \vec{\nabla}\vartheta|^{-1}$ is the Jacobian and $\mathcal{E}(\omega)$ is related to the wave energy. Thus, Eq. (4) requires that wave energy be finite. To be more specific, in Eq. (3), r and ϑ are, respectively, a radial-like flux coordinate and a poloidal-like angle, and perturbations have $\approx \exp(in\varphi)$ dependence in the toroidal angle φ. For simplicity, we also assume that r and ϑ are chosen such that equilibrium magnetic field lines are straight on a given flux surface.

In the following, we demonstrate that one can construct eigenmode solutions of Eq. (3) by solving two nested one-dimensional ordinary differential equations rather than Eq. (3) itself. The advantage of this approach is obvious, since solving an ordinary differential equation is much simpler than tackling a partial differential problem and, perhaps more importantly, the underlying physics also emerges more clearly. Qualitatively, the solution of the two nested one-dimensional differential equations is equivalent to first solving for the mode structure along the field lines locally and then constructing the two-dimensional global mode structure through a superposition of local solutions. Since the procedure outlined below is quite general, we consider a wide class of operators that can lead to Eq. (3).

Since the toroidal equilibrium is periodic in the poloidal angle ϑ, the solution $\delta\phi$ and the operator $\mathcal{D}$ of Eq. (3) must also be periodic, i.e.,

$$\delta\phi(\omega; r, \vartheta + 2\pi) = \delta\phi(\omega; r, \vartheta) ,$$

$$\mathcal{D}(\omega; r, \vartheta + 2\pi, \partial_r, \partial_\vartheta) = \mathcal{D}(\omega; r, \vartheta, \partial_r, \partial_\vartheta) .$$

Thus, we can represent the perturbation $\delta\phi(\omega; r, \vartheta)$ and the operator $\mathcal{D}(\omega; r, \vartheta, \partial_r, \partial_\vartheta)$ as Fourier series

$$\delta\phi(\omega; r, \vartheta) = \sum_m e^{-im\vartheta} \delta\phi_m(\omega; r) ,$$

$$\mathcal{D}(\omega; r, \vartheta, \partial_r, \partial_\vartheta) = \sum_\ell e^{i\ell\vartheta} \mathcal{D}_\ell(\omega; r, \partial_r, \partial_\vartheta) .$$

Equation (3) can then be rewritten as

$$\sum_\ell \sum_j e^{-ij\vartheta} \mathcal{D}_\ell\left(\omega; r, \partial_r, -i(j+\ell)\right) \phi_{j+\ell}(\omega; r) = 0 ,$$

where $j = m - \ell$, or, equivalently, as

$$\sum_\ell \mathcal{D}_\ell\left(\omega; r, \partial_r, -i(j+\ell)\right) \phi_{j+\ell}(\omega; r) = 0 . \qquad (5)$$

Equation (5) has transformed the original two-dimensional eigenvalue problem, Eq. (3), into an infinite set of coupled one-dimensional differential equations.

In the high-n limit, each Fourier harmonic $\delta\phi_m$ tends to have a highly localized structure around the surface $r_o^{(m)}$, where $nq(r_o^{(m)}) = m$. This is because the most important perturbations have parallel (to the ambient magnetic field) wavelengths $\approx qR$; which are much larger than perpendicular ones $\approx O(a/n)$. Furthermore, the equilibrium properties do not appreciably change from a rational surface $r_o^{(m)}$ to the next $r_o^{(m+1)}$. As a consequence, the Fourier harmonics $\delta\phi_m$ are expected to have similar shapes, slowly changing throughout the plasma column along with their amplitude A_m. In other words, the $\delta\phi_m$'s can be assumed to have the form

$$\delta\phi_m(\omega; r) = A_m\phi(m, nq - m) = A(nq)\phi(nq, nq - m) , \qquad (6)$$

where the *fast* variable $nq - m$ accounts for the rapid radial variations, which determine the localized self-similar shape of the poloidal harmonics $\delta\phi_m$, while the *slow* variable nq describes the changes in the *shape functions* $\phi(nq, nq - m)$ and in the amplitudes $A(nq)$ on a scale determined by equilibrium nonuniformities. Typically, $|\partial \ln \phi(nq, nq-m)/\partial(nq-m)| = O(1)$, while $|\partial \ln \phi(nq, nq-m)/\partial(nq)| \approx |\partial \ln A(nq)/\partial(nq)| = O(1/n\delta)$, where δ is a parameter depending on the particular wave mode to be studied and on the details of the chosen plasma equilibrium. This separation of scales is crucial to treating the two-dimensional problem with a WKB approach; as suggested first in Ref. [25] and Ref. [26].

The dependence of the operators $\mathcal{D}_\ell(\omega; r, \partial_r, -i(j + \ell))$ in Eq. (5) on the radial coordinate r is reflected in dependences on both fast $nq-m$ and slow nq normalized radial variables. In general, the dependence on $nq - m$ enters to account for parallel variations ($k_{\|m,n} = (nq - m)/qR$), while nq describes other radial equilibrium

nonuniformities. Thus

$$\mathcal{D}_\ell\left(\omega; r, \partial_r, -i(j+\ell)\right) \rightarrow \mathcal{D}_\ell\left(\omega; nq, nq-j-\ell, \partial_r, -i(j+\ell)\right) \ .$$

Furthermore, the localization of the various poloidal harmonics implies $j+\ell \simeq nq$; i.e.,

$$\mathcal{D}_\ell\left(\omega; nq, nq-j-\ell, \partial_r, -i(j+\ell)\right) \rightarrow \hat{\mathcal{D}}_\ell\left(\omega; nq, nq-j-\ell, \partial_r\right) \ . \tag{7}$$

For convenience, we also assume that it is possible to write

$$\hat{\mathcal{D}}_\ell\left(\omega; nq, nq-j-\ell, \partial_r\right) = \sum_p \hat{\mathcal{D}}_{\ell,p}\left(\omega; nq, nq-j-\ell\right) \partial_r^p \ ;$$

Equation (5) then becomes

$$\sum_{\ell,p} \hat{\mathcal{D}}_{\ell,p}\left(\omega; nq, nq-j-\ell\right) \partial_r^p \phi_{j+\ell}(\omega; r) = 0 \ . \tag{8}$$

The existence of two separate scales allows us to write the shape function $\phi(nq, nq-m)$ as

$$\phi(nq, nq-m) \equiv \phi(t, nq-m) = \int_{-\infty}^{+\infty} e^{-i(nq-m)\theta} \Phi(t,\theta) d\theta \ , \tag{9}$$

where $t \equiv nq$ has been used as a short notation for the slow normalized radial variable. The condition Eq. (4) legislates that $\Phi(t,\theta)$ be square integrable, such that the integral in Eq. (9) is well defined. This constraint has frequently led to the remark that the description of the local radial shape of the single Fourier harmonics by means of the dual variable θ (also referred to as the extended poloidal angle, or ballooning coordinate[25]) were inadequate in the case of *singular* eigenfunctions, typical of a continuous spectrum. This observation appears to be further confirmed by the breakdown of the *translational invariance* of the shape functions $\phi(t, nq-m)$ in the transition from regular harmonics of a discrete spectrum to

singular harmonics of a continuum. This, however, is not the case. The only basic assumption underlying Eq. (9) is the existence of two characteristic scale lengths. In fact, employing the causality constraint and the proper analytic continuation, Eq. (9) can represent both regular as well as "singular" poloidal harmonics. This point will be explicitly shown in Section IV.A for the case of TAE modes. This result, however, is very general and indicates that the "ballooning transform" of Eq. (9) can be used to analyze the coupling between high-n discrete and continuous spectra.

As to the amplitudes $A(nq) \equiv A(t)$, we adopt the following eikonal representation

$$A(t) = \exp\left(i \int^t \theta_k(t')dt'\right) . \tag{10}$$

Here, the notation $\theta_k(t)$ was originally proposed in Ref. [26] for the local normalized radial wave vector $-(i/n)\partial/\partial q$. Equations (9) and (10), along with Eq. (6), allow us to rewrite $\delta\phi_m(\omega; r)$ as

$$\delta\phi_m(\omega; r) = e^{i\int^t \theta_k(t')dt'} \int_{-\infty}^{+\infty} e^{-i(nq-m)\theta} \Phi(t,\theta)d\theta , \tag{11}$$

which is the form used in Ref. [20]. Substituting Eq. (11) into Eq. (8), we have

$$\sum_{\ell,p} e^{i\ell\theta} \hat{\mathcal{D}}_{\ell,p}(\omega; t, -i\partial_\theta)\, i^p \left[nq'(\theta_k(t) - \theta - i\partial_t)\right]^p \Phi(t,\theta) = 0 . \tag{12}$$

In Eq. (12), $|\theta_k(t)| \approx |\theta| \approx 1$ reflects the rapidly varying local structure of the shape functions $\phi(t, nq-m)$ on the scale $\approx 1/nq'$, while $|\partial_t \ln\theta_k(t)| \approx |\partial_t \ln\Phi(t,\theta)| \approx 1/n\delta$ account for the changes of the shape function and of the amplitude $A(t)$ on a scale $\approx \delta/q' \approx \delta a$. Here, we have assumed that the local flux surface averaged magnetic shear $s = rq'/q$ is an $O(1)$ quantity. The case of vanishing shear must be handled with some care, since q can not be used as a radial variable in this case.

Equation (12) can be solved by asymptotically expanding the various quantities in the smallness parameter $1/n\delta$; e.g., $\theta_k(t) = \theta_k^{(0)}(t) + \theta_k^{(1)}(t) + \ldots$. To the lowest order, assume we can solve the one-dimensional boundary value problem in the variable θ

$$\sum_{\ell,p} e^{i\ell\theta} \hat{\mathcal{D}}_{\ell,p}\left(\omega; t, -i\partial_\theta\right) i^p \left[nq'\left(\theta_k^{(0)}(t) - \theta\right)\right]^p \Phi^{(0)}(t,\theta) = 0 \ , \tag{13}$$

with boundary conditions $|\Phi^{(0)}(t,\theta)| \to 0$ as $|\theta| \to \infty$, leading to the constraint

$$L\left(\omega; t, \theta_k^{(0)}(t)\right) = 0 \ . \tag{14}$$

This local constraint is a *local dispersion relation*, which gives the implicit form of the lowest order WKB phase $\theta_k^{(0)}(t)$, or, equivalently, establishes a relationship between the normalized local wave vector $\theta_k^{(0)}$ and the mode frequency ω. Note that, because of Eq. (13), $L\left(\omega; t, \theta_k^{(0)}(t)\right)$ is a periodic function of $\theta_k^{(0)}$ of period 2π. This fact is naturally demonstrated using $\theta' = \theta - \theta_k^{(0)}(t)$ as a new ballooning coordinate and noting that the dependences on $\theta_k^{(0)}(t)$ in Eq. (13) would be then only in the terms $e^{i\ell\theta_k^{(0)}(t)}$.

In the following, we will restrict our analysis to differential operators satisfying the symmetry property

$$\int_{-\infty}^{+\infty} d\theta \Psi(t,\theta) \sum_{\ell,p} e^{i\ell\theta} \hat{\mathcal{D}}_{\ell,p}\left(\omega; t, -i\partial_\theta\right) i^p \left[nq'\left(\theta_k(t) - \theta\right)\right]^p \Phi(t,\theta) =$$
$$= \int_{-\infty}^{+\infty} d\theta \Phi(t,\theta) \sum_{\ell,p} e^{i\ell\theta} \hat{\mathcal{D}}_{\ell,p}\left(\omega; t, -i\partial_\theta\right) i^p \left[nq'\left(\theta_k(t) - \theta\right)\right]^p \Psi(t,\theta) \ . \tag{15}$$

From Eq. (13), we can construct the following quadratic form

$$F\left(\omega; t, \theta_k^{(0)}\right) = \int_{-\infty}^{+\infty} d\theta \, \Phi^{(0)}(t,\theta) \sum_{\ell,p} e^{i\ell\theta}$$
$$\hat{\mathcal{D}}_{\ell,p}\left(\omega; t, -i\partial_\theta\right) i^p \left[nq'\left(\theta_k^{(0)}(t) - \theta\right)\right]^p \Phi^{(0)}(t,\theta) = 0 \ . \tag{16}$$

Note that, in constructing Eq. (16), one needs to integrate in θ by parts and apply the proper boundary conditions.

Clearly, Eq. (16) is equivalent to Eq. (14), i.e.,

$$L\left(\omega; t, \theta_k^{(0)}(t)\right) \sim F\left(\omega; t, \theta_k^{(0)}(t)\right) = 0 \ , \tag{17}$$

when the differential operator of Eq. (13) is symmetric. In this case, in fact, it is possible to show that the differential equation Eq. (13) admits a *variational principle* in the form of Eq. (16).[31] Note that symmetry is much weaker than hermiticity and, in particular, it does not require that the considered system is non-dissipative.

The relation of the phase trajectories $\theta_k^{(0)}(t)$ to the radial profile of the local dispersion function is shown in Fig.4. There, a phase space "libration"[32] around an O-point corresponds to a local minimum of $F(\theta_k^{(0)}, \Omega_o^2, \alpha, s)$: this is because, for the reference case of TAE's, $\partial F/\partial\theta_k^{(0)} > 0$ for $0 < \theta_k^{(0)} < \pi$; $\partial F/\partial\theta_k^{(0)} < 0$ would yield the opposite. Phase space "rotations"[32] (open trajectories), in general, correspond to the monotonic branches of $F(\theta_k^{(0)}, \Omega_o^2, \alpha, s)$.[24]

To the next order in the $1/n\delta$ expansion, the corresponding quadratic form becomes

$$\int_{-\infty}^{+\infty} d\theta \int\int_{-\infty}^{+\infty} d\xi d\xi' e^{-it(\xi+\xi')} \hat{\Phi}^{(0)}(\xi', \theta) \sum_{\ell,p} e^{i\ell\theta} i^p p \hat{\mathcal{D}}_{\ell,p}\left(\omega; t, -i\partial_\theta\right)$$
$$\left\{ -\left[nq'\left(\theta_k^{(0)}(t) - \theta\right)\right]^{p-1} nq' \frac{\xi+\xi'}{2} - i\frac{p-1}{2}\left[nq'\left(\theta_k^{(0)}(t) - \theta\right)\right]^{p-2}\left[nq'\partial_t\theta_k^{(0)}(t) + \right.\right.$$
$$\left.\left. + nq''\left(\theta_k^{(0)} - \theta\right)\right] + \left[nq'\left(\theta_k^{(0)}(t) - \theta\right)\right]^{p-1} nq'\theta_k^{(1)}(t)\right\} \hat{\Phi}^{(0)}(\xi, \theta) = 0 \ ; \tag{18}$$

where, for convenience, we have used the Fourier representation of the function $\Phi^{(0)}(t, \theta)$

$$\Phi^{(0)}(t, \theta) = \int_{-\infty}^{+\infty} e^{-it\xi} \hat{\Phi}^{(0)}(\xi, \theta) d\xi \ ,$$

and the symmetry property of Eq. (15) has been used to replace $\xi \to (\xi + \xi')/2$ in the first term in the curly brackets and to eliminate $\Phi^{(1)}(\omega; t, \theta)$. From Eq. (18), one finds

$$\theta_k^{(1)} = \frac{i}{2}\frac{d}{dt}\ln\frac{\partial}{\partial\theta_k^{(0)}}F\left(\omega; t, \theta_k^{(0)}(t)\right) \quad ; \tag{19}$$

where the $\partial_t\hat{\mathcal{D}}_{\ell,p}\left(\omega; t, -i\partial_\theta\right)$ have been neglected because of the slow equilibrium variations. The general WKB expression of the radial envelope function is thus

$$A(t) \sim \frac{\text{const}}{\sqrt{\partial F/\partial\theta_k^{(0)}}}\exp i\int^t \theta_k^{(0)}(t')dt' \ . \tag{20}$$

Moreover, note that $\partial_t\theta_k^{(0)}$ tends to become singular at a WKB turning point position $(t_T, \theta_{kT}^{(0)})$, where $\partial F/\partial\theta_k^{(0)} = 0$. Locally, one therefore needs to solve the following differential equation

$$\left\{\frac{1}{2}\left.\frac{\partial^2 F}{\partial\theta_k^{(0)2}}\right|_{(t_T,\theta_{kT}^{(0)})}\left(-i\partial_t - \theta_{kT}^{(0)}\right)^2 + F\left(\omega; t, \theta_{kT}^{(0)}\right) - F\left(\omega; t_T, \theta_{kT}^{(0)}\right)\right\}A(t) = 0 \ , \tag{21}$$

to derive the corresponding WKB connection formulae. In Eq. (21) $\partial^2 F/\partial\theta_k^{(0)2}|_{(t_T,\theta_{kT}^{(0)})} \neq 0$ is assumed. Equation (21) can be readily obtained by constructing from Eq. (12) a "quadratic form" and then Taylor expanding around the turning point position.

We remark that Eq. (20) has a clear physical interpretation for the case of a dissipationless system, where the maximum order of the $\hat{\mathcal{D}}_{\ell,p}\left(\omega; t, -i\partial_\theta\right)$ operators is $\ell = p = 2$. Then, $\partial_\omega F \sim U(\omega; t)$, the wave energy density.[33] In the absence of dissipation, the energy flux is constant, i.e.,

$$v_g(\omega; t)U(\omega; t)|A(t)|^2 = -\frac{\partial F/\partial\theta_k^{(0)}}{\partial F/\partial\omega}\frac{\partial F}{\partial\omega}|A(t)|^2 \sim \text{const} \ , \tag{22}$$

where $v_g(\omega; t)$ is the normalized group velocity of the wave. Equation (22) is consistent with Eq. (20).

Applying the connection formulae to the WKB solutions given by Eq. (20) along with the proper boundary conditions, the WKB *global dispersion relation* for the eigenmode frequency is obtained in terms of quantization conditions (cf. Section IV.B).

We note that the present formalism differs from the previous well-known approaches of Refs. [25–27] in that our treatment of the local mode structure along the magnetic field lines allows us to handle singular eigenfunctions of the continuum. That is, the translational invariance of the shape functions $\phi(t, nq - m)$ can now be extended into the continuous spectrum by means of analytic continuation. A second important difference is in the analysis of the radial eigenmode structure. The standard ballooning approach[25,34,35] assumes closely spaced turning points. Equation (21) is then solved near an extremum $\partial F/\partial t = 0$ for localized solutions corresponding to the phase space librations of Fig.4. The eigenmodes have typical radial extent $\Delta r \approx a/n^{1/2}$ and the global mode frequency differs from the local one by an $O(1/n)$ term.[25] Meanwhile, the present interpretation of θ_k as a normalized local radial wave-vector treats also the eigenmodes corresponding to phase space rotations (open trajectories of Fig.4). In general, these eigenmodes have rather extended radial mode structures and are characterized by well separated turning point pairs. In fact, $\Delta r \approx \delta a$ with δ being independent of n. The existence of eigenmodes with spaced turning points is also emphasized in Ref. [26] and Ref. [36] but not treated in detail; the attention there being rather focused on the case of closely spaced turning points due to the nature of the ideal ballooning instabilities.

Briefly summarizing this Section, we have formulated a theoretical approach for analyzing two-dimensional eigenmode structures of high-n modes in axisymmetric

toroidal equilibria. The wave-operators $\mathcal{D}(\omega; r, \vartheta, \partial_r, \partial_\vartheta)$ of Eq. (3) are general and are required to satisfy only the symmetry property of Eq. (15). In Ref. [36], it is pointed out that operators obtained in the analysis of kinetic ballooning modes are symmetric. The present approach is then amenable not only to analyses of the coupling between discrete and continuous spectra, but also of other non-ideal and kinetic effects. Other interesting applications could be the in the extension of previous studies of high-n toroidal drift waves[34,35] to the radially extended modes with well-spaced turning points mentioned above.[37,38] Finally, it may be interesting to extend the validity of the present formalism to low-n perturbations. In this case, we may adopt a procedure essentially equivalent to the formal construction of a Fourier Integral Operator for the radial eigenmode structure.[39] Work along this direction will be reported in a future publication.

In the next Sections, we will apply the theoretical formalism presented here to the particular case of TAE modes. We will also use the fact that the wave absorption rate is expected to be small compared to the frequency gap width, i.e. $|\omega_i| << \epsilon_o \omega_A/2$, to perturbatively compute the TAE continuum damping. While formally not necessary, the perturbative calculation does reduce some mathematical complexities and, thus, make the physical picture more transparent. In addition, for practical purposes the small damping rate limit is also the relevant case to study.

III. Eigenmode Equations

The governing equations for TAE's can be derived from the quasi-neutrality condition $\vec{\nabla} \cdot \delta\vec{J} = 0$; i.e.,

$$\vec{\nabla} \cdot \delta\vec{J}_\perp + \vec{B} \cdot \vec{\nabla} \left(\frac{\delta J_\parallel}{B} \right) = 0 \ , \tag{23}$$

where $\delta \vec{J}$ is the perturbed current, and $\perp$ and $\parallel$ refer, respectively, to the perpendicular and parallel directions with respect to the equilibrium magnetic field vector $\hat{b} \equiv \vec{B}/B$. The expression for $\delta J_\parallel$ is given by the parallel Ampére's law

$$4\pi\delta J_\parallel = c\hat{b} \cdot \vec{\nabla} \times \left(\vec{\nabla} \times \delta\vec{A} \right) \ ,$$

$\delta\vec{A}$ being the perturbed vector potential. Thus, in an axisymmetric toroidal equilibrium,

$$\delta J_\parallel = -\frac{c}{4\pi} \nabla_\perp^2 \delta A_\parallel \left(1 + O\left(\frac{a}{nR_o} \right) \right) \ . \tag{24}$$

Here, n is the toroidal mode number. $\delta A_\parallel$ can be further expressed in terms of the electrostatic potential perturbation $\delta\phi$ via the parallel Ohm's law $\delta E_\parallel = 0$; i.e.,

$$-\hat{b} \cdot \vec{\nabla}\delta\phi + i\frac{\omega}{c}\delta A_\parallel = 0 \ .$$

Note that time dependence of the form $\approx \exp(-i\omega t)$ has been assumed.

The perpendicular current perturbation is obtained from the perpendicular force balance; i.e.,

$$\begin{aligned} \delta\vec{J}_\perp \ = \ & \frac{c}{B^2} \vec{B} \times \varrho \frac{\partial}{\partial t} \delta\vec{v}_\perp + \frac{c}{B^2} \vec{B} \times \vec{\nabla}\delta p + \\ & + \frac{J_\parallel}{B} \delta\vec{B}_\perp - \frac{\delta B_\parallel}{B} \frac{c}{B^2} \vec{B} \times \vec{\nabla} P \ . \end{aligned} \tag{25}$$

Here, P is the equilibrium pressure and $\beta \equiv 8\pi P/B^2 = O(\epsilon_o)$. In Eq. (25), the perpendicular velocity $\delta\vec{v}_\perp$, meanwhile, is given by the Ohm's law

$$\vec{B} \times \delta\vec{v}_\perp = -c\vec{\nabla}_\perp \delta\phi \ ; \tag{26}$$

and the pressure perturbation δp by the equation of state

$$-i\omega\,\delta p + \delta\vec{v}_\perp \cdot \vec{\nabla} P \simeq 0 \ , \tag{27}$$

or

$$\delta p = \frac{c}{i\omega}\frac{\vec{B}\times\vec{\nabla}_\perp\delta\phi}{B^2}\cdot\vec{\nabla}P \simeq \left(\frac{ck_\perp}{\omega B}\right)\frac{\partial P}{\partial\Psi}\Psi'\,\delta\phi \ , \tag{28}$$

where $k_\perp$ is the wave vector component orthogonal to $\hat{b}$ and the magnetic flux surface labeled by Ψ. In Eq. (27), the $\gamma P(\vec{\nabla}\cdot\delta\vec{v})$ compression term can be shown to give negligible $O(\epsilon_o)$ and $O(\epsilon_o\beta)$ corrections. From Eq. (25), we then find

$$\left(1+O\left(\frac{1}{n}\right)\right)\vec{\nabla}\cdot\delta\vec{J}_\perp = i\vec{\nabla}\cdot\left[\frac{c^2}{B^2}\varrho\omega\vec{\nabla}_\perp\delta\phi\right] - 2c\vec{\kappa}\times\frac{\vec{B}}{B^2}\cdot\vec{\nabla}_\perp\delta p - \\ - c\,\frac{\vec{B}\times\vec{\nabla}P}{B^4}\cdot\vec{\nabla}_\perp\left(4\pi\delta p + B\delta B_{||}\right) \ ,$$

where $\vec{\kappa} \equiv \hat{b}\cdot\vec{\nabla}\hat{b}$ is the magnetic field curvature.

For $n >> 1$ the fluctuations are localized in the radial direction, i.e. their typical width is much smaller than the minor radius of the torus. Moreover the modes considered here are characterized by the shear Alfvén time scale; which is much longer (an order $O(nR_o/a)$) than that of the compressional Alfvén wave. As a consequence,

$$4\pi\delta p + B\delta B_{||} = 0 \tag{29}$$

to the lowest order in n, which expresses the perpendicular pressure balance. This allows us to further simplify the expression of $\vec{\nabla} \cdot \delta \vec{J}_\perp$.

Combining Eqs. (24) through (29), Eq. (23) can be cast into the form of the following vorticity equation

$$B\hat{b} \cdot \vec{\nabla} \left[\frac{1}{B} \nabla_\perp^2 \hat{b} \cdot \vec{\nabla} \delta\phi \right] + \vec{\nabla} \cdot \left[\frac{4\pi\varrho}{B^2} \omega^2 \vec{\nabla}_\perp \delta\phi \right] - \\ -8\pi\vec{\kappa} \times \frac{\vec{B}}{B^2} \cdot \vec{\nabla}_\perp \left[\left(\frac{\vec{B} \times \vec{\nabla} P}{B^2} \right) \cdot \vec{\nabla}_\perp \delta\phi \right] = 0 \ . \qquad (30)$$

Equation (30) can be also derived as the Euler-Lagrange equation from the following Lagrangian

$$\delta L = \int d\vec{r} \left\{ \left| \vec{\nabla}_\perp \hat{b} \cdot \vec{\nabla} \delta\phi \right|^2 - \frac{\omega^2}{v_A^2} \left| \vec{\nabla}_\perp \delta\phi \right|^2 + \right. \\ \left. +8\pi\vec{\kappa} \times \frac{\vec{B}}{B^2} \cdot \vec{\nabla}_\perp \delta\phi^* \quad \frac{\vec{B} \times \vec{\nabla} P}{B^2} \cdot \vec{\nabla}_\perp \delta\phi \right\} . \qquad (31)$$

Here, only internal modes are considered. Equations (30) and (31) are, of course, completely equivalent.

In axisymmetric tokamaks, Eq. (30) is a two-dimensional partial differential equation; which can be solved, with the proper boundary conditions, as an eigenvalue problem for the complex frequency ω using the approach outlined in Section II. The damping rate ω_i due to the mode coupling to the continuous shear Alfvén spectrum and the TAE radial eigenmode structure are, thus, completely determined.

We can, nevertheless, use additional information to further simplify the problem. The fact that the damping rate is expected to be small, i.e., $|\omega_i| << \epsilon_o \omega_A/2$,

suggests using perturbation techniques to compute the wave absorption rate. This can be readily done using a variational principle, which is the approach adopted in this work. Thus, for the practical purpose, we can use the theoretical formulation of Section II for the two-dimensional eigenmode analysis of TAE modes neglecting the coupling to the shear Alfvén continuous spectrum (cf. Section IV) and then, to the next order in the perturbative expansion, use Eq. (31) to derive a general expression for the continuum damping rate (cf. Section V).

Our aim is to solve Eq. (30) in the high-n limit, using a local finite-β axisymmetric equilibrium for a large aspect ratio tokamak with shifted circular magnetic flux surfaces.[28] This represents a simplified and yet relevant case to study for TAE modes when the magnetic flux surfaces are weakly shaped. Thus, for simplicity, we shall consider such a model equilibrium, even though our approach can be readily extended to include effects due to non-circularity of the magnetic flux surfaces, like ellipticity, triangularity etc. .[29]

For convenience, we work with flux coordinates in which the equilibrium magnetic field lines are straight. Specifically, we choose the curvilinear coordinate system (r, φ, ϑ), where r is a radial-like flux function, φ is the toroidal angle, and ϑ is a poloidal-like angle, chosen such that the Jacobian $J \equiv \left(\vec{\nabla}\vartheta \times \vec{\nabla}r \cdot \vec{\nabla}\varphi\right)^{-1} = R^2 r/R_o$.[24] Because of the shift of the circular magnetic surfaces, $r = r_o + d(1 + \Delta' \cos\vartheta) + ...$, Δ' being the derivative of the Shafranov shift, r_o being defined by $nq(r_o) = m_o$, the central poloidal mode number, and d being the distance from the reference flux surface at r_o.

The perturbation $\delta\phi$ can be written in the form[23,24]

$$\delta\phi = \exp\{i\,[n\varphi + m_o(r - r_o)\alpha \sin\vartheta/r_o]\}\, e^{-im_o\vartheta} \sum_j \delta\phi_j(r)\, e^{-ij\vartheta} \quad , \qquad (32)$$

where, we recall, $\alpha = -R_o q^2 \beta'$. In Section I, we already emphasized that, even though TAE modes are expected to have rather extended radial structures $\Delta r_{TAE} \approx \epsilon_o L_A$, they are carachterized by a small spread in the excited poloidal mode numbers; i.e., $|j| = O(\epsilon_o |m_o|)$ in Eq. (32), so that m_o may be regarded as the "central" mode number. We can then define the slow normalized radial coordinate t, introduced in Section II, as $t \equiv (r - r_o)/\Delta r_s$, Δr_s being the distance between two neighbouring rational surfaces, i.e., $\Delta r_s \equiv 1/nq'(r_o)$. The fast normalized radial variable $nq - m$, thus, becomes $nq - m = t - j$. With $\delta\phi$ expressed as in Eq. (32), the gradient operator along the equilibrium magnetic field lines varies only on the connection length scale:

$$\hat{b} \cdot \vec{\nabla} = \frac{i}{qR}[n(q - q_o) - j] = \frac{i}{qR}(t - j) \ . \tag{33}$$

The eigenmode equations are obtained by substituting Eq. (32) into the vorticity equation, Eq. (30). After some tedious algebra,[24] it is possible to show that the TAE eigenmode equations are given by

$$\begin{aligned}
& s^2 \frac{\partial}{\partial t}\left[(t-j)^2 - \Omega^2\right]\frac{\partial}{\partial t}\delta\phi_j - \left[(t-j)^2 - \Omega^2\right]\delta\phi_j + \\
& + s\alpha(t-j)\frac{\partial}{\partial t}\Big[(t-j-1)\delta\phi_{j+1} - (t-j+1)\delta\phi_{j-1}\Big] + \\
& + \frac{\alpha^2}{4}(t-j)\Big[(t-j-2)\delta\phi_{j+2} - 2(t-j)\delta\phi_j + (t-j+2)\delta\phi_{j-2}\Big] - \\
& - s\alpha\Omega^2\frac{\partial}{\partial t}(\delta\phi_{j+1} - \delta\phi_{j-1}) - \frac{\alpha^2}{4}\Omega^2(\delta\phi_{j+2} - 2\delta\phi_j + \delta\phi_{j-2}) + \\
& + \frac{\alpha}{2}\left[\delta\phi_{j+1} + \delta\phi_{j-1} + s\frac{\partial}{\partial t}(\delta\phi_{j+1} - \delta\phi_{j-1})\right] + \\
& + \frac{\alpha^2}{4}(\delta\phi_{j+2} - 2\delta\phi_j + \delta\phi_{j-2}) =
\end{aligned}$$

$$= \epsilon_o \Omega^2 \left[\left(s^2 \frac{\partial^2}{\partial t^2} - 1 \right) (\delta\phi_{j+1} + \delta\phi_{j-1}) + s\alpha \frac{\partial}{\partial t} (\delta\phi_{j+2} - \delta\phi_{j-2}) + \right.$$
$$\left. + \frac{\alpha^2}{4} (\delta\phi_{j+3} - \delta\phi_{j+1} - \delta\phi_{j-1} + \delta\phi_{j-3}) \right] . \qquad (34)$$

Here, $\epsilon_o \equiv 2(r_o/R_o + \Delta')$ is the strength of toroidal coupling and $\Omega = qR_o^2\omega/v_A R$ is the mode frequency normalized to the local Alfvén frequency.

Similarly, employing Eq. (32), the Lagrangian of Eq. (31) can be rewritten as:

$$\frac{\delta L}{2\pi R_o} = \kappa_\vartheta^2 \frac{2\pi r_o \Delta r_s}{q^2 R_o^2} \int dt \sum_j \left\{ s^2 \left[(t-j)^2 - \Omega^2 \right] \left| \frac{\partial}{\partial t} \delta\phi_j \right|^2 + \right.$$
$$+ \left[(t-j)^2 - \Omega^2 \right] |\delta\phi_j|^2 + \frac{\alpha^2}{2} \left[(t-j)^2 - \Omega^2 + 1 \right] |\delta\phi_j|^2 -$$
$$- s\alpha(t-j) \left[\delta\varphi_j^* \frac{\partial}{\partial t} ((t-j-1)\delta\phi_{j+1}) + c.c. \right] +$$
$$+ s\alpha \left(\Omega^2 - \frac{1}{2} \right) \left[\delta\phi_j^* \frac{\partial}{\partial t} \delta\phi_{j+1} + c.c. \right] - \frac{\alpha}{2} \left(\delta\phi_j^* \delta\phi_{j+1} + c.c. \right) -$$
$$- \frac{\alpha^2}{4} \left[(t-j)(t-j-2) - \Omega^2 + 1 \right] \left(\delta\phi_j^* \delta\phi_{j+2} + c.c. \right) -$$
$$- \epsilon_o \Omega^2 \left[s^2 \frac{\partial}{\partial t} \delta\phi_j^* \frac{\partial}{\partial t} \delta\phi_{j+1} + \delta\phi_j^* \delta\phi_{j+1} - s\alpha \delta\phi_j^* \frac{\partial}{\partial t} \delta\phi_{j+2} - \right.$$
$$\left. \left. - \frac{\alpha^2}{4} \left(\delta\phi_j^* \delta\varphi_{j+3} - \delta\phi_j^* \delta\phi_{j+1} \right) + c.c. \right] \right\} . \qquad (35)$$

Here, $k_\vartheta \equiv m_o/r_o$ is the central poloidal wave vector of the excited mode. In Eqs. (34) and (35), Ω^2, α and s are functions of the slow radial variable t due to equilibrium inhomogeneities. Such a dependence can be more explicitly displayed by introducing profile functions for Ω^2, α and s; i.e., by letting $\Omega^2 \equiv \bar{\Omega}^2 f(t)$, $\alpha \equiv \bar{\alpha} g(t)$ and $s \equiv \bar{s} h(t)$, with $f(0) = g(0) = h(0) = 1$. Also ϵ_o, in general, can be a function of t. In the following it will be assumed constant in order to reduce the algebra, but the approach presented here is sufficiently general such that this assumption could be relaxed straightforwardly.

IV. Two-Dimensional Eigenmode Analysis

In this Section, we will use the approach outlined in Section II to explicitly compute the lowest order two-dimensional eigenmode structure of TAE modes. That is, we shall neglect the coupling to the continuous shear Alfvén spectrum and assume undamped TAE modes ($\Omega = \Omega_o + i\gamma \Rightarrow \Omega_o$).

The existence of the fast and slow radial scales, $t - j$ and t, suggests that the poloidal harmonics $\delta\phi_j$ be expressed as, cf. Eqs. (6) and (11),

$$\begin{aligned} \delta\phi_j(t) &= A(t)\,\phi(t, t-j) = \\ &= e^{i\int^t \theta_k(t')dt'} \int_{-\infty}^{+\infty} d\theta\, e^{-i(t-j)\theta}\, \Phi(t,\theta) \ . \end{aligned} \tag{36}$$

A. TAE Local Dispersion Relation

Substituting Eq. (36) into Eq. (34), the lowest-order one-dimensional eigenmode equation in θ is then given by

$$\begin{aligned} \left[\frac{\partial}{\partial\theta}\left(1+I_o^2\right)\frac{\partial}{\partial\theta}\right. &+ \Omega_o^2\left(1+I_o^2\right)(1+2\epsilon_o\cos\theta) + \\ &+ \left.\alpha\left(\cos\theta + I_o\sin\theta\right)\right]\Phi(t,\theta) = 0 \ , \end{aligned} \tag{37}$$

with

$$I_o = s\left(\ell - \theta_k^{(0)}\right) - \alpha\sin\theta \ . \tag{38}$$

Letting $\delta\psi = \sqrt{1+I_o^2}\,\Phi^{(0)}(t,\theta)$, Eq. (37) can be rewritten as

$$\left[\frac{\partial^2}{\partial\theta^2} + \Omega_o^2\left(1+2\epsilon_o\cos\theta\right) - \frac{(s-\alpha\cos\theta)^2}{\left(1+I_o^2\right)^2} + \frac{\alpha\cos\theta}{1+I_o^2}\right]\delta\psi = 0 \ . \tag{39}$$

The solution of Eq. (39) with boundary conditions $|\delta\psi| \to 0$ as $|\theta| \to \infty$ leads to the local dispersion relation for TAE modes.

For convenience, let θ' be the shifted variable $\theta' \equiv \theta - \theta_k^{(0)}$. In the 'External Region' $|s\theta'| >> \mathrm{Max}(1,\alpha)$, Eq. (39) becomes a Mathieu equation

$$\left[\frac{\partial^2}{\partial\theta^2} + \Omega_o^2\left(1 + 2\epsilon_o \cos(\theta + \theta_k^{(0)})\right)\right] \delta\psi_E = 0 \ , \tag{40}$$

where, from now on, the prime in θ' will be dropped. From the general solution of the Mathieu equation, it is well known that curves exist in the (ϵ_o, Ω_o^2) plane, which separate regions in which the asymptotic behaviour of the solutions is exponentially increasing or decreasing, from regions in which the asymptotic behaviour is oscillatory. In the $\epsilon_o << 1$ limit, these critical curves are given by $\Omega_o^2 = (1 \pm \epsilon_o)/4$. Using the ordering $|\Omega_o^2 - 1/4| \approx \epsilon_o$, Eq. (40) can be solved perturbatively[6] as

$$\delta\psi_E = A(\theta) \cos\left(\frac{\theta + \theta_k^{(0)}}{2}\right) + B(\theta) \sin\left(\frac{\theta + \theta_k^{(0)}}{2}\right) \ , \tag{41}$$

where $A(\theta)$ and $B(\theta)$ vary on the slow scale $\theta \approx 1/\epsilon_o$. Substituting Eq. (41) into Eq. (40), and averaging over the $\theta \approx O(1)$ fast scale,[6] one derives the following coupled equations

$$\begin{aligned} B(\theta)' + \Gamma_+ A(\theta) &= 0 \ , \\ -A(\theta)' + \Gamma_- B(\theta) &= 0 \ ; \end{aligned}$$

where

$$\Gamma_\pm = \left(\Omega_o^2 - \frac{1}{4}\right) \pm \epsilon_o \Omega_o^2 \ . \tag{42}$$

Then, we have

$$\begin{aligned} A(\theta)^{(\pm)} &= a^{(\pm)} (-\Gamma_-)^{1/2} e^{\mp\hat{\gamma}\theta} \ , \\ B(\theta)^{(\pm)} &= \pm a^{(\pm)} (\Gamma_+)^{1/2} e^{\mp\hat{\gamma}\theta} \ . \end{aligned}$$

Here, the $\pm$ sign refers, respectively, to positive and negative values of θ, $a^{(\pm)}$ are arbitrary constants, and

$$\hat{\gamma} = (-\Gamma_- \Gamma_+)^{1/2} = \sqrt{\epsilon_o^2 \Omega_o^4 - \left(\Omega_o^2 - \frac{1}{4}\right)^2} \quad . \tag{43}$$

From Eq. (43), we see that, for $|\Omega_o^2 - 1/4| < \epsilon_o \Omega_o^2$, the asymptotic behaviour of $\delta\psi_E^{(\pm)}$ is exponentially decaying, which means that the Fourier Transform of Eq. (36) is well defined. For $|\Omega_o^2 - 1/4| \geq \epsilon_o \Omega_o^2$, the expression for $\hat{\gamma}$ must be analytically continued, such that unstable modes decay in θ fast enough, and Eq. (36) remains well defined. This leads to

$$\hat{\gamma} \rightarrow -i\,|\hat{\gamma}|\,\frac{\Omega_o}{|\Omega_o|}\,\frac{\Omega_o^2 - 1/4}{|\Omega_o^2 - 1/4|} \quad , \quad \text{for} \quad |\Omega_o^2 - 1/4| \geq \epsilon_o \Omega_o^2 \ . \tag{44}$$

In real space, the $|\Omega_o^2 - 1/4| < \epsilon_o \Omega_o^2$ condition corresponds to the regular poloidal harmonics of the discrete spectrum, while the singular structure, which appears for $|\Omega_o^2 - 1/4| \geq \epsilon_o \Omega_o^2$, is that of the poloidal harmonics of the continuous spectrum (cf. Appendix A). The expression of $\delta\psi_E$, thus, becomes

$$\delta\,\psi_E^{(\pm)} = a^{(\pm)} \left[\sqrt{-\Gamma_-} \cos\left(\frac{\theta + \theta_k^{(0)}}{2}\right) \pm \sqrt{\Gamma_+} \sin\left(\frac{\theta + \theta_k^{(0)}}{2}\right) \right] e^{\mp \hat{\gamma}\theta} \ . \tag{45}$$

That the expression given by Eq. (45) is valid for $|\Omega_o^2 - 1/4| \geq \epsilon_o \Omega_o^2$, i.e. inside the continuous spectrum, is of crucial importance. In fact, using arguments based on causality constraints, the ballooning approach can be generalized to handle both regular and singular (unnormalizable) poloidal harmonics; i.e., to simultaneously describe discrete and continuous MHD spectra. Although only the lowest-order two-dimensional eigenvalue problem for the undamped TAE is analyzed here, this fact is important since it allows us to derive the eigenmode structure and the local

dispersion relation at the continuum resonances. In this respect, by means of the Fourier Transform of the Ballooning Eigenfunction (see Appendix B), we will be able to find the singular behaviour of the poloidal harmonics of the continuous spectrum at the resonances (see Appendix A). This is achieved, of course, with the proper analytic continuation of $\hat{\gamma}$ based on causality arguments.

In the 'Internal Region' $|\epsilon_o \theta| << 1$, $O(\epsilon_o)$ terms in Eq. (39) are negligible. Equation (39) then reduces to

$$\left[\frac{\partial^2}{\partial\theta^2} + \frac{1}{4} + \frac{\alpha\cos(\theta+\theta_k^{(0)})}{1+p^2} - \frac{\left(s-\alpha\cos(\theta+\theta_k^{(0)})\right)^2}{(1+p^2)^2}\right]\delta\psi_I = 0 \ , \qquad (46)$$

where

$$p = s\theta - \alpha\sin(\theta+\theta_k^{(0)}) \ . \qquad (47)$$

Assume now that we can find the independent solutions of Eq. (46). This can be done analytically for asymptotic values of the parameters and, in general, numerically.[24] In the overlapping region between 'Internal' and 'External' regions, $\mathrm{Max}(1,\alpha)/s << |\theta| << 1/\epsilon_o$, the asymptotic behaviour of the independent solutions of Eq. (46) is $\cos(\theta/2)$ or $\sin(\theta/2)$. At $\theta = 0$, the values of the asymptotic solution $\approx \cos(\theta/2)$ and of its first derivative are $\delta\psi_c^{(\pm)}(\theta_k^{(0)},s,\alpha)$ and $\delta\psi_c^{(\pm)\prime}(\theta_k^{(0)},s,\alpha)$. Because of the symmetry of Eq. (46) under the parity transformation $(\theta \to -\theta; \theta_k^{(0)} \to -\theta_k^{(0)})$, we have

$$\begin{aligned}\delta\psi_c^{(+)}(\theta_k^{(0)},s,\alpha) &\equiv \delta\psi_c \ , \\ \delta\psi_c^{(-)}(\theta_k^{(0)},s,\alpha) &= \delta\psi_c^{(+)}(-\theta_k^{(0)},s,\alpha) \equiv \delta\bar{\psi}_c \ ,\end{aligned}$$

$$
\begin{aligned}
\delta\psi_c^{(+)\prime}(\theta_k^{(0)},s,\alpha) &\equiv \delta\psi_c' \ , \\
\delta\psi_c^{(-)\prime}(\theta_k^{(0)},s,\alpha) &= -\delta\psi_c^{(+)\prime}(-\theta_k^{(0)},s,\alpha) \equiv -\delta\bar{\psi}_c' \ .
\end{aligned} \tag{48}
$$

Analogously, for the asymptotic solution $\approx \sin(\theta/2)$, we find

$$
\begin{aligned}
\delta\psi_s^{(+)}(\theta_k^{(0)},s,\alpha) &\equiv \delta\psi_s \ , \\
\delta\psi_s^{(-)}(\theta_k^{(0)},s,\alpha) &= -\delta\psi_s^{(+)}(-\theta_k^{(0)},s,\alpha) \equiv -\delta\bar{\psi}_s \ , \\
\delta\psi_s^{(+)\prime}(\theta_k^{(0)},s,\alpha) &\equiv \delta\psi_s' \ , \\
\delta\psi_s^{(-)\prime}(\theta_k^{(0)},s,\alpha) &= \delta\psi_s^{(+)\prime}(-\theta_k^{(0)},s,\alpha) \equiv \delta\bar{\psi}_s' \ .
\end{aligned} \tag{49}
$$

The 2π periodicity in $\theta_k^{(0)}$ of Eq. (46) gives the same periodicity to the functions defined in Eqs. (48) and (49). Using these results, the solutions of Eq. (46), which asymptotically match $\delta\psi_E^{(\pm)}$ of Eq. (45), assume the following expressions at $\theta = 0$:

$$
\begin{aligned}
\delta\psi_I^{(+)}(0) &= a^{(+)}\left\{\left[\sqrt{-\Gamma_-}\delta\psi_c + \sqrt{\Gamma_+}\delta\psi_s\right]\cos\left(\frac{\theta_k^{(0)}}{2}\right) + \right. \\
&\quad \left. + \left[\sqrt{\Gamma_+}\delta\psi_c - \sqrt{-\Gamma_-}\delta\psi_s\right]\sin\left(\frac{\theta_k^{(0)}}{2}\right)\right\} \ , \\
\delta\psi_I^{(+)\prime}(0) &= a^{(+)}\left\{\left[\sqrt{-\Gamma_-}\delta\psi_c' + \sqrt{\Gamma_+}\delta\psi_s'\right]\cos\left(\frac{\theta_k^{(0)}}{2}\right) + \right. \\
&\quad \left. + \left[\sqrt{\Gamma_+}\delta\psi_c' - \sqrt{-\Gamma_-}\delta\psi_s'\right]\sin\left(\frac{\theta_k^{(0)}}{2}\right)\right\} \ ;
\end{aligned} \tag{50}
$$

$$
\delta\psi_I^{(-)}(0) = a^{(-)}\left\{\left[\sqrt{-\Gamma_-}\delta\bar{\psi}_c + \sqrt{\Gamma_+}\delta\bar{\psi}_s\right]\cos\left(\frac{\theta_k^{(0)}}{2}\right) + \right.
$$

$$+\left[-\sqrt{\Gamma_+}\delta\bar{\psi}_c+\sqrt{-\Gamma_-}\delta\bar{\psi}_s\right]\sin\left(\frac{\theta_k^{(0)}}{2}\right)\Bigg\}\ ,$$

(51)

$$\delta\psi_l^{(-)\prime}(0) = a^{(-)}\left\{-\left[\sqrt{-\Gamma_-}\delta\bar{\psi}_c'+\sqrt{\Gamma_+}\delta\bar{\psi}_s'\right]\cos\left(\frac{\theta_k^{(0)}}{2}\right)+\right.$$
$$\left.+\left[\sqrt{\Gamma_+}\delta\bar{\psi}_c'-\sqrt{-\Gamma_-}\delta\bar{\psi}_s'\right]\sin\left(\frac{\theta_k^{(0)}}{2}\right)\right\}\ .$$

The 'Internal Solutions' of Eq. (46), given by Eqs. (50) and (51), must match at $\theta = 0$. This leads to the following local dispersion relation

$$F\left(\theta_k^{(0)},\Omega_o^2,\alpha,s\right) \equiv Z(\theta_k^{(0)},s,\alpha)\,\hat{\gamma}+2\,G(\theta_k^{(0)},s,\alpha)\,(\Omega_o^2-1/4)+ \tag{52}$$
$$+2\,\epsilon_o\Omega_o^2\left(H(\theta_k^{(0)},s,\alpha)\cos\theta_k^{(0)}+L(\theta_k^{(0)},s,\alpha)\sin\theta_k^{(0)}\right)=0\,;$$

where

$$\begin{aligned}
Z &= \left(\delta\psi_c\delta\bar{\psi}_s'+\delta\psi_s\delta\bar{\psi}_c'+\delta\psi_s'\delta\bar{\psi}_c+\delta\psi_c'\delta\bar{\psi}_s\right)\ ,\\
G &= \frac{1}{2}\left(\delta\psi_s\delta\bar{\psi}_s'-\delta\psi_c\delta\bar{\psi}_c'+\delta\psi_s'\delta\bar{\psi}_s-\delta\psi_c'\delta\bar{\psi}_c\right)\ ,\\
H &= \frac{1}{2}\left(\delta\psi_s\delta\bar{\psi}_s'+\delta\psi_c\delta\bar{\psi}_c'+\delta\psi_s'\delta\bar{\psi}_s+\delta\psi_c'\delta\bar{\psi}_c\right)\ ,\\
L &= \frac{1}{2}\left(\delta\psi_c\delta\bar{\psi}_s'-\delta\psi_s\delta\bar{\psi}_c'-\delta\psi_s'\delta\bar{\psi}_c+\delta\psi_c'\delta\bar{\psi}_s\right)\ ,
\end{aligned} \tag{53}$$

and $Z^2 = 1+4(H^2-G^2+L^2)$. Equation (52) and (53) indicate that to determine the explicit dependence of $F(\theta_k^{(0)},\Omega_o^2,\alpha,s)$ on s, α and $\theta_k^{(0)}$, one needs only to solve Eq. (46). This task is considerably simpler than the original problem given by Eq. (39) and, furthermore, can be solved numerically. Finally, noting that Z, G, H are even and L is odd in $\theta_k^{(0)}$, Eq. (52), the local dispersion relation, is then even in $\theta_k^{(0)}$, reflecting the up-down symmetry of the equilibrium.

B. The Global Radial Eigenvalue Problem

Here, we shall employ the WKB technique to analyze the next-order global radial eigenmode problem. In the case of $F(\theta_k^{(0)}, \Omega_o^2, \alpha, s)$ being a monotonic function of t, one can show that there are two turning points, $t = t_T^{(1)}$ and $t = t_T^{(2)}$, inside the frequency gap.[24] The envelope function decays exponentially outside the turning points. This makes $A(t)$ itself exponentially small for the poloidal harmonics of the continuous spectrum. As a consequence, the resonant damping of the mode is small; justifies, thus, a perturbative calculation. Defining $x = a_1 t$ with $a_1 \equiv -[(\partial F/\partial t)/(\partial^2 F/\partial \theta_k^{(0)2})]_{t=t_T^{(1)}}$, we find,[24] for $x < x_T^{(1)}$,

$$A^{(-)}(x) = \frac{K\, e^{i\pi/4 + ik\pi - i\pi x_T^{(1)}/|a_1|}}{\sqrt{\partial F/\partial \theta_k^{(0)}}} \exp\left[-i \int_{x_T^{(1)}}^{x} \frac{\theta_k^{(0)}}{|a_1|}\, dx\right] , \tag{54}$$

K being an arbitrary constant, and k the radial quantum number. For $x_T^{(1)} < x < x_T^{(2)}$,

$$A^{(o)}(x) = \frac{2\,K}{\sqrt{\partial F/\partial \theta_k^{(0)}}} \sin\left[\int_{x}^{x_T^{(2)}} \frac{\theta_k^{(0)}}{|a_1|}\, dx + \frac{\pi}{4}\right] ; \tag{55}$$

and, finally, for $x > x_T^{(2)}$,

$$A^{(+)}(x) = \frac{K\, e^{i\pi/4}}{\sqrt{\partial F/\partial \theta_k^{(0)}}} \exp\left[i \int_{x_T^{(2)}}^{x} \frac{\theta_k^{(0)}}{|a_1|}\, dx\right] . \tag{56}$$

Here, $\pi \geq \theta_k^{(0)} \geq 0$ for $x_T^{(1)} \leq x \leq x_T^{(2)}$, while $\theta_k^{(0)} = \pi + i\Im\theta_k^{(0)}$ for $x < x_T^{(1)}$ and $\theta_k^{(0)} = i\Im\theta_k^{(0)}$ for $x > x_T^{(2)}$ (the imaginary part of $\theta_k^{(0)}$, $\Im\theta_k^{(0)} \geq 0$ in both cases) in the gap region. The global dispersion relation for Ω_o is given by[24]

$$\int_0^{\pi} t(\theta_k^{(0)}, \Omega_o^2, s, \alpha)\, d\theta_k^{(0)} = k\pi \qquad k \in Z , \tag{57}$$

which is the quantization condition for the area enclosed by the phase trajectory $t(\theta_k^{(0)})$ and the $\theta_k^{(0)}$ axis in the $(\theta_k^{(0)}, t)$ plane, as shown in Fig.5.

Equations (54) to (57) represent general results in the case of a monotonic variation of $F(\theta_k^{(0)}, \Omega_o^2, \alpha, s)$ with t. In principle, we could solve the local dispersion relation (which is a transcendental function) for $\theta_k^{(0)}$ as a function of t. However, the phase integrals in the WKB expression of the envelope $A(t)$ and the quantization condition must, in general, be computed numerically.

The typical global radial width of the envelope function and, therefore, of the mode is $\Delta r_{TAE} \approx \epsilon_o L_A$. This is consistent with the assumption of radial mode localization ($\Delta r_{TAE} << a$) and with the possibility of solving the problem with a two-scale expansion scheme, since $\Delta r_{TAE} >> \Delta r_s$, the typical distance between rational surfaces.

The case of a local parabolic profile of $F(\theta_k^{(0)}, \Omega_o^2, \alpha, s)$ (i.e. $\partial F/\partial t|_{t=t_T} = 0$ and $\partial^2 F/\partial t^2|_{t=t_T} \neq 0$) can be treated in the same way and gives $\Delta r \approx \epsilon_o^{1/4} r_o (L_A/n r_o)^{1/2}$. It is thus less interesting (and less general) than the case considered here.

It is also worthwhile to note that the presence of mode structures having short poloidal wavelength patterns ($k_\vartheta \sim m_o/r_o$) with, however, a rather extended global radial width $\Delta r \approx \epsilon_o L_A$ may have interesting implications for transport issues.[37,38]

V. Variational Formulation and Resonant Damping

Substituting the poloidal harmonics $\delta\phi_j$ expressed in Eq. (36) into the Lagrangian of Eq. (35), the variational formulation of the TAE eigenvalue problem reduces to

$$\delta L_{NR} + i\delta L_R = 0 \ .$$

Here, δL_{NR} is the *nonresonant component* of the Lagrangian, due to the contribution of the regular Fourier harmonics excited within the gap region (cf. Fig.3); while the imaginary term, the *resonant Lagrangian* δL_R, comes from the contribution to Eq. (35) due to the singular poloidal harmonics excited in the continuous shear Alfvén spectrum. The lowest order real eigenfrequency Ω_o clearly gives $\delta L_{NR}(\Omega_o) \equiv 0$, identically. The nonresonant Lagrangian can be written as

$$\frac{\delta L_{NR}}{2\pi R_o} = k_\vartheta^2 \frac{2\pi r_o \Delta r_s}{q^2 R_o^2} 2\pi \int_{-\infty}^{+\infty} dt |A(t)|^2 \delta \hat{L}_{NR} \ ; \tag{58}$$

where $A(t)$ is the envelope function given by Eqs. (54) through (56), and

$$\delta \hat{L}_{NR} = \int_{-\infty}^{+\infty} d\theta \left\{ \left| \frac{\partial}{\partial \theta} \delta\psi \right|^2 - \left[\Omega_o^2 \left(1 + 2\epsilon_o \cos(\theta + \theta_k^{(0)}) \right) - \right. \right.$$
$$\left. \left. - \frac{\left(s - \alpha \cos(\theta + \theta_k^{(0)}) \right)^2}{(1+p^2)^2} + \frac{\alpha \cos(\theta + \theta_k^{(0)})}{(1+p^2)} \right] |\delta\psi|^2 \right\} \ .$$

In the next order, we calculate the resonant Lagrangian δL_R to derive the general expression for the TAE continuum damping

$$\frac{\gamma}{\Omega_o} = - \frac{\delta L_R}{2\Omega_o^2 \partial L_{NR}/\partial \Omega_o^2} \ . \tag{59}$$

It is interesting to note that Eq. (59) can be also derived from energy conservation.[24]

Because of the singular layer ordering (cf. Appendix A), $\partial/\partial t \approx 1/\epsilon_o$, only quadratic terms in the radial derivatives need to be kept to evaluate the leading-order δL_R; i.e.,

$$\begin{aligned}\frac{i\,\delta\,L_R}{2\pi R_o} &= k_\vartheta^2 \frac{2\pi r_o \Delta r_s}{q^2 R_o^2}\, s^2 \sum_\ell \int dx \left[\left(x^2 - \Omega_o^2\right) |\partial_x\, \delta\,\phi_\ell|^2 + \right. \\ &+ \left((x-1)^2 - \Omega_o^2 \right) |\partial_x\, \delta\,\phi_{\ell+1}|^2 - \\ &- \left. \epsilon_o \Omega_o^2 \left(\partial_x\, \delta\phi_\ell^*\, \partial_x\, \delta\,\phi_{\ell+1} + c.c. \right) \right] . \end{aligned} \tag{60}$$

In Eq. (60) $x \equiv (t - \ell)$, and the sum is over all resonances, and the 'ℓth' resonance consists of contributions due to the poloidal harmonics ℓ and $\ell+1$ (cf. Fig.2). The expressions for $\partial_x \delta\phi_\ell^{(0)}$ and $\partial_x \delta\phi_{\ell+1}^{(0)}$ can be obtained solving the truncated two-mode Eq. (34) for $x \to 1/2$. We then find (see Appendix A)

$$\frac{\partial}{\partial x}\,\delta\,\phi_\ell^{(0)} = \frac{B_\ell \left((x-1)^2 - \Omega_o^2\right) + \epsilon_o\, \Omega_o^2\, C_\ell}{D_\ell} , \tag{A.4}$$

$$\frac{\partial}{\partial x}\,\delta\,\phi_{\ell+1}^{(0)} = \frac{C_\ell \left(x^2 - \Omega_o^2\right) + \epsilon_o\, \Omega_o^2\, B_\ell}{D_\ell} , \tag{A.5}$$

$$D_\ell = \left(x^2 - \Omega_o^2\right) \left((x-1)^2 - \Omega_o^2\right) - \epsilon_o^2\, \Omega_o^4 . \tag{A.6}$$

By substitution of Eqs. (A.4) to (A.6) into Eq. (60), the integrand there becomes

$$\begin{aligned}[...] &= \frac{1}{D_\ell^*} \left\{ |B_\ell|^2 \left[(x-1)^2 - \Omega_o^2\right]^* + |C_\ell|^2 \left(x^2 - \Omega_o^2\right)^* + \right. \\ &+ \left. \left(\epsilon_o \Omega_o^2\right)^* \left(B_\ell C_\ell^* + B_\ell^* C_\ell\right) \right\} . \end{aligned} \tag{61}$$

Note that in Eq. (61) correct complex conjugate operations have been explicitly carried out in order to satisfy the causality constraint and properly define analytic

continuation in the complex Ω_o plane. Thus, letting $\Omega_o \rightarrow \Omega_o + i\Delta$ with Ω_o real and $\Delta > 0$, we have

$$D_\ell^* = \left((x-1)^2 - \Omega_o^2\right)\left(x^2 - \Omega_o^2\right) - \epsilon_o^2\Omega_o^4 + \\ + 2i\Omega_o\Delta\left[\left(x^2 - \Omega_o^2\right) + \left((x-1)^2 - \Omega_o^2\right) + 2\epsilon_o^2\Omega_o^2\right] .$$

For $\Omega_o = \pm 1/2 + \delta\Omega_o$ and $x = 1/2 + \delta x$, we have

$$D_\ell^* = \left(\delta\Omega_o^2 - \delta x^2 - \frac{\epsilon_o^2}{16}\right) - 2i\Delta\delta\Omega_o .$$

Outside the 'gap region', where the resonances with the continuous shear Alfvén spectrum occur, $\delta\Omega_o^2 > \epsilon_o^2/16$ and the equation $D_\ell^* = 0$ can be solved for $\delta x = \delta x_r + i\delta x_i$, with

$$\delta x = \pm\lambda_\ell \mp i\Delta\frac{\delta\Omega_o}{\lambda_\ell} ,$$

λ_ℓ being given by the expression

$$\lambda_\ell = \sqrt{\delta\Omega_o^2 - \frac{\epsilon_o^2}{16}} = \sqrt{\left(\Omega_o^2 - \frac{1}{4}\right)^2 - \epsilon_o^2\Omega_o^4} . \qquad (62)$$

Thus, we can write

$$D_\ell^* = -\left[\left(\delta x - \lambda_\ell + i\Delta\frac{\delta\Omega_o}{\lambda_\ell}\right)\left(\delta x + \lambda_\ell - i\Delta\frac{\delta\Omega_o}{\lambda_\ell}\right)\right] .$$

Due to the resonant structure of the denominator in the integrand of Eq. (60), the integral picks up an imaginary part coming from the residues of the simple poles. The resonant Lagrangian of Eq. (60) becomes thus

$$\frac{i\,\delta\,L_R}{2\pi R_o} = k_\vartheta^2 \frac{2\pi r_o \Delta r_s}{q^2 R_o^2}\,(\,-i\pi s^2\,)\sum_\ell \frac{2\Omega_o\,|\delta\,\Omega_o|}{\lambda_\ell}\,\Big[\,|B_\ell|^2 + |C_\ell|^2 - \frac{\epsilon_o\,\Omega_o}{2\,\delta\,\Omega_o}\,(B_\ell^*\,C_\ell + B_\ell\,C_\ell^*)\Big]\ . \tag{63}$$

Note that the expressions for B_ℓ and C_ℓ can be derived (cf. Appendix B) via the matching of the solution of the truncated two-mode Euler Lagrange equations, Eqs. (A.1), with the Fourier Transform of the ballooning eigenfunctions, and are given by Eqs. (B.7). As discussed thereafter, B_ℓ and C_ℓ are independent on the normalization function $N(t)$ chosen for the ballooning eigenfunction $\Phi^{(0)}(t,\theta)$. A particularly convenient choice for $N(t)$[24] allows us to rewrite Eq. (63) as

$$\frac{i\,\delta\,L_R}{2\pi R_o} = k_\vartheta^2\,\frac{2\pi r_o \Delta r_s}{q^2 R_o^2}\,\frac{\Omega_o}{|\Omega_o|}\,(-2i\pi)\sum_\ell \lambda_\ell\,|A_\ell|^2\ . \tag{64}$$

With the same normalization, one can explicitly show that

$$\delta\,\hat{L}_{NR} = -\,F(\theta_k^{(0)}, \Omega_o^2, \alpha, s)\ , \tag{65}$$

where $F(\theta_k^{(0)}, \Omega_o^2, \alpha, s)$ is the local dispersion function of Eq. (52). This identity demonstrates the consistency of the two approaches, as it should.

Substituting Eqs. (65) and (64), along with Eq. (58), into Eq. (59), we obtain the following general expression for the TAE mode damping rate due to finite coupling with the continuous shear Alfvén spectrum

$$\frac{\gamma}{|\Omega_o|} = -\,\frac{\sum_\ell \lambda_\ell\,|A_\ell|^2}{2\Omega_o^2 \dfrac{\partial}{\partial \Omega_o^2}\displaystyle\int_{-\infty}^{+\infty} |A(t)|^2\,F(\theta_k^{(0)}, \Omega_o^2, \alpha, s)\,dt}\ . \tag{66}$$

Here, we note that $\partial/\partial\Omega_o^2$ acts only on the $F(\theta_k^{(0)}, \Omega_o^2, \alpha, s)$. In the high mode number limit, $n\epsilon_o >> 1$, Eq. (66) is generally valid and requires only knowing

the envelope function $A(t)$ and the local dispersion function. On the other hand, Equations (54) through (56) are valid for $F(\theta_k^{(0)}, \Omega_o^2, \alpha, s)$ varying monotonically with t. Similar analytic expressions can be derived for a local parabolic profile of the dispersion function. However, in the most general case, the phase integrals appearing in the WKB expression of the radial envelope, the quantization condition, Eq. (57), and the damping rate, Eq.(66), must be computed numerically.

VI. Resonant Damping for a Linear Ω_o^2 Profile

In the following, in order to make further analytic progress, we specialize to the case of a linear Ω_o^2 profile; i.e. $\Omega_o^2 = \bar{\Omega}_o^2(1 + at)$, where

$$a \equiv \frac{\Delta r_s}{L_A} = \frac{1}{nq'(r_o)L_A} = \frac{r_o}{nq(r_o)sL_A} , \tag{67}$$

$$L_A \equiv \left| \frac{\partial}{\partial r} \ln\left(\frac{q^2\varrho}{B^2X^2}\right) \right|^{-1} , \tag{68}$$

with α and s constant. In particular, employing for $A(t)$ the WKB expression of Eq. (55), the denominator of Eq. (66) becomes

$$I\left(\Omega_o^2, s, \alpha\right) = \int_{t_<}^{t_>} 8\,\Omega_o^2\,|K|^2\,\frac{\partial F/\partial\Omega_o^2}{\left|\partial F/\partial\theta_k^{(0)}\right|}\,\sin^2\left(\int_x^{x_T^{(2)}} \frac{\theta_k^{(0)}}{|a_1|}\,dx' + \frac{\pi}{4}\right) dt .$$

Here, $t_<$ and $t_>$ refer to the two turning points coordinates and exponentially small contributions outside the turning points have been neglected. Due to the fast (relative to the scale length of $F(\theta_k^{(0)}, \Omega_o^2, \alpha, s)$, i.e., of the equilibrium) oscillations of the phase integral appearing in the previous expression, we can replace the sinusoidal function with its average value, i.e., $\sin^2(...) = 1/2$. Moreover, from the local dispersion relation, we have

$$\frac{d\theta_k^{(0)}}{dt} = -\frac{a}{|a|}\left|\frac{d\theta_k^{(0)}}{dt}\right| ,$$

and

$$\frac{\partial F}{\partial t} = \frac{a}{|a|}\left|\frac{\partial F}{\partial t}\right| .$$

Noting that

$$\frac{d\theta_k^{(0)}}{dt} = -\frac{\partial F/\partial t}{\partial F/\partial\theta_k^{(0)}}$$

and changing the integration variable from t to $\theta_k^{(0)}$, we have

$$I\left(\Omega_o^2, s, \alpha\right) = 4\,|K|^2 \int_0^\pi \frac{d\theta_k^{(0)}}{|a|} = \frac{4\pi}{|a|}\,|K|^2 \;; \tag{69}$$

that is, Eq. (66) becomes

$$\frac{\gamma}{|\Omega_o|} = -\frac{|a|}{4\pi|K|^2} \sum_\ell \lambda_\ell\,|A_\ell|^2 \;. \tag{70}$$

To go further, we first note that Z, G, H and L are periodic functions in $\theta_k^{(0)}$. The local dispersion relation, Eq. (52), can thus be conveniently expressed as a Fourier series; i.e.

$$\begin{aligned} F\left(\theta_k^{(0)}, \Omega_o^2, \alpha, s\right) \;\equiv\; & Z(\theta_k^{(0)}, s, \alpha)\,\hat{\gamma} + 2\,G(\theta_k^{(0)}, s, \alpha)\,(\Omega_o^2 - 1/4) \;+ \\ & +2\,\epsilon_o\Omega_o^2\;(\;H(\theta_k^{(0)}, s, \alpha)\,\cos\,\theta_k^{(0)} \;+\; L(\theta_k^{(0)}, s, \alpha)\,\sin\,\theta_k^{(0)}\;) \;= \\ = \sum_{m=-1}^{\infty} & \;[\,Z_m(s,\alpha)\,\hat{\gamma} \;+\; 2\,G_m(s,\alpha)\,\left(\Omega_o^2 - 1/4\right) \;+\; \epsilon_o\Omega_o^2\,(H_{m-1}(s,\alpha) \;+ \\ & \;+\; H_{m+1}(s,\alpha) + \;L_{m+1}(s,\alpha) - L_{m-1}(s,\alpha))]\,\cos m\theta_k^{(0)} \;=\; 0 \;. \end{aligned} \tag{71}$$

Here, the subscript m denotes the mth Fourier component and all quantities are meant to vanish for negative values of their index.

In the gap region, between the WKB turning points, $0 \le \theta_k^{(0)} \le \pi$, $\theta_k^{(0)} = \pi$ corresponding to the turning point $t_T^{(1)}$ closer to the lower shear Alfvén continuous spectrum ($\Omega_o^2(1+\epsilon_o) \le 1/4$); and $\theta_k^{(0)} = 0$ corresponding to $t_T^{(2)}$, closer to the upper continuum ($\Omega_o^2(1-\epsilon_o) \ge 1/4$). In the exponentially decaying regions outside $t_T^{(1)}$ and $t_T^{(2)}$ but inside the gap, $\theta_k^{(0)}$ has constant real part and picks up a positive imaginary part. Finally, in the upper continuum, we have $\theta_k^{(0)} \equiv \beta_k^{(+)}\frac{\Omega_o}{|\Omega_o|} + i\eta_k^{(+)}$;

and, in the lower continuum, $\theta_k^{(0)} \equiv \pi - \beta_k^{(-)} \frac{\Omega_o}{|\Omega_o|} + i\eta_k^{(-)}$. Here, $\beta_k^{(\pm)}$ and $\eta_k^{(\pm)}$ are positive definite phases which can be calculated from the local dispersion relation Eq. (52). The resonance with the continuum occurs at $at \geq at_{R(+)}$ (upper) and $at \leq at_{R(-)}$ (lower), with

$$at_{R(\pm)} = -1 \pm \epsilon_o + \frac{1}{4\bar{\Omega}_o^2} .$$

The summation in Eq. (70) can be further approximated as (let $y \equiv at$)

$$\sum_\ell \lambda_\ell |A_\ell|^2 = \int_{-\infty}^{at_{R(-)}} \frac{\lambda^{(-)}(y)}{|a|} \left|A^{(-)}(y)\right|^2 dy + \\ + \int_{at_{R(+)}}^{\infty} \frac{\lambda^{(+)}(y)}{|a|} \left|A^{(+)}(y)\right|^2 dy ; \qquad (72)$$

where

$$\lambda^{(\pm)}(y) = \sqrt{\bar{\Omega}_o^4 \left(y - y_{R(\pm)}\right)^2 \pm 2\epsilon_o \bar{\Omega}_o^4 \left(y - y_{R(\pm)}\right)} , \qquad (73)$$

and $A^{(\pm)}$ are given by the WKB expressions of Eq. (56) and Eq. (54). In the present form, Eq. (72) is still analytically intractable. To approximate it further, we note that the envelope function is exponentially decaying and, thus, the dominant wave absorption occurs near $y_{R(\pm)}$. We can then approximate

$$A^{(-)}(y) \simeq \frac{K e^{i\pi/4 + ik\pi - i\pi y/|a|}}{\sqrt{\partial F/\partial \theta_k^{(0)}\big|_{y_{R(-)}}}} \exp\left(-T + \frac{\theta_{k(-)}^{(0)}}{|a|}\left(y - y_{R(-)}\right)\right) , \qquad (74)$$

$$A^{(+)}(y) \simeq \frac{K e^{i\pi/4}}{\sqrt{\partial F/\partial \theta_k^{(0)}\big|_{y_{R(+)}}}} \exp\left(-R - \frac{\theta_{k(+)}^{(0)}}{|a|}\left(y - y_{R(+)}\right)\right) , \qquad (75)$$

and

$$\lambda^{(\pm)}(y) \simeq \bar{\Omega}_o^2 \sqrt{\pm 2\epsilon_o \left(y - y_{R(\pm)}\right)} \ . \tag{76}$$

Here, $\theta^{(0)}_{k(\pm)}(s,\alpha)$ are the values of the imaginary part of $\theta^{(0)}_k$ at the resonance points $t_{R(\pm)}$, i.e. they are solutions of

$$\sum_{m=-1}^{\infty} (\pm 1)^m \left[\pm 2G_m + (H_{m-1} + H_{m+1}) + \right.$$
$$\left. + (L_{m+1} - L_{m-1}) \right] \cosh m\theta^{(0)}_{k(\pm)} = 0 \ .$$

The tunneling factors T and R, meanwhile, determine the strength of the mode coupling to the continuous shear Alfvén spectrum, and are given by

$$T = \int_{y_{R(-)}}^{y_T^{(1)}} \frac{\Im\theta^{(0)}_k}{|a|} dy \quad \text{and} \quad R = \int_{y_T^{(2)}}^{y_{R(+)}} \frac{\Im\theta^{(0)}_k}{|a|} dy \ . \tag{77}$$

Noting Eq. (71), we can also write

$$\left| \left. \frac{\partial F}{\partial \theta^{(0)}_k} \right|_{y_{R(\pm)}} \right| = \epsilon_o \bar{\Omega}_o^2 \, P_{(\pm)} \ ,$$

with

$$P_{(\pm)} = \left| \sum_{m=-1}^{\infty} (\pm 1)^m \, m \left[\pm 2G_m + (H_{m-1} + H_{m+1}) + \right. \right.$$
$$\left. \left. + (L_{m+1} - L_{m-1}) \right] \sinh m\theta^{(0)}_{k(\pm)} \right| \ .$$

The resonant damping rate, Eq. (59), can then be approximated as

$$\frac{\gamma}{|\Omega_o|} = -\frac{|a|^{3/2}}{16\,\pi^{1/2}\epsilon_o^{1/2}} \left\{ \frac{\exp(-2T)}{P_{(-)}\,\theta^{(0)3/2}_{k(-)}} + \frac{\exp(-2R)}{P_{(+)}\,\theta^{(0)3/2}_{k(+)}} \right\} \ . \tag{78}$$

Explicit expressions of T and R can be obtained from Eq. (77), changing the integration variable from y to $\theta_k^{(0)}$, along with the local dispersion relation, Eq. (52),[24] and the results are

$$T = \frac{\epsilon_o}{|a|}\theta^{(0)}_{k(-)} - \frac{\epsilon_o}{|a|}\int_0^{\theta^{(0)}_{k(-)}} dx\ \frac{4G\left(H\cos\theta_k^{(0)} + L\sin\theta_k^{(0)}\right)}{(Z^2+4G^2)}\Bigg|_{\theta_k^{(0)}=\pi+ix} + \tag{79}$$

$$+ \frac{\epsilon_o}{|a|}\int_{\theta^{(0)}_{k(-)}}^{\bar\theta^{(0)}_{k(-)}} dx\ \frac{|Z|}{(Z^2+4G^2)}\left[Z^2+4G^2-4\left(H\cos\theta_k^{(0)} + L\sin\theta_k^{(0)}\right)^2\right]^{1/2}_{\theta_k^{(0)}=\pi+ix}$$

$$- \frac{\epsilon_o}{|a|}\int_0^{\bar\theta^{(0)}_{k(-)}} dx\ \frac{Z}{(Z^2+4G^2)}\left[Z^2+4G^2-4\left(H\cos\theta_k^{(0)} + L\sin\theta_k^{(0)}\right)^2\right]^{1/2}_{\theta_k^{(0)}=\pi+ix}$$

$$R = \frac{\epsilon_o}{|a|}\theta^{(0)}_{k(+)} + \frac{\epsilon_o}{|a|}\int_0^{\theta^{(0)}_{k(+)}} dx\ \frac{4G\left(H\cos\theta_k^{(0)} + L\sin\theta_k^{(0)}\right)}{(Z^2+4G^2)}\Bigg|_{\theta_k^{(0)}=+ix} + \tag{80}$$

$$+ \frac{\epsilon_o}{|a|}\int_{\theta^{(0)}_{k(+)}}^{\bar\theta^{(0)}_{k(+)}} dx\ \frac{|Z|}{(Z^2+4G^2)}\left[Z^2+4G^2-4\left(H\cos\theta_k^{(0)} + L\sin\theta_k^{(0)}\right)^2\right]^{1/2}_{\theta_k^{(0)}=+ix}$$

$$+ \frac{\epsilon_o}{|a|}\int_0^{\bar\theta^{(0)}_{k(+)}} dx\ \frac{Z}{(Z^2+4G^2)}\left[Z^2+4G^2-4\left(H\cos\theta_k^{(0)} + L\sin\theta_k^{(0)}\right)^2\right]^{1/2}_{\theta_k^{(0)}=+ix}$$

Here, $\bar\theta^{(0)}_{k(\pm)}(s,\alpha)$ is the solution of the equation

$$\left[Z^2 + 4G^2 - 4\left(H\cos\theta_k^{(0)} + L\sin\theta_k^{(0)}\right)^2\right]_{\theta_k^{(0)}=i\bar\theta^{(0)}_{k(\pm)}+(1/2\mp1/2)\pi} = 0\ .$$

VII. Limiting Cases and Numerical Results

A. Zero-Pressure ($\alpha = 0$) case

With $\alpha = 0$, one can show from Eq. (46) that only the zeroth Fourier harmonics of Z, G and H contribute to the local dispersion relation.[20,21] One finds $\theta^{(0)}_{k(\pm)} = \operatorname{arccosh}|G_o/H_o|$, $\bar{\theta}^{(0)}_{k(\pm)} = \operatorname{arccosh}(1/\kappa)$,$\kappa^2 = 4H_o^2/(Z_o^2 + 4G_o^2)$, and $P_{(\pm)} = 2|H_o|\sinh\theta^{(0)}_{k(\pm)} = 2\sqrt{G_o^2 - H_o^2}$. Equations (78) to (80) then reduce to

$$\frac{\gamma}{|\Omega_o|} = -\frac{|a|^{3/2}}{32\sqrt{\pi}\sqrt{\epsilon_o G_o^2}} \frac{\left[\operatorname{arccosh}\left|\frac{G_o}{H_o}\right|\right]^{-3/2}}{\sqrt{1 - \frac{H_o^2}{G_o^2}}} [\exp(-2T) + \exp(-2R)] \ , \qquad (81)$$

where

$$\begin{aligned} T &= \frac{\epsilon_o}{|a|}\operatorname{arccosh}\left|\frac{G_o}{H_o}\right| + \frac{\epsilon_o}{|a|}\frac{G_o}{H_o}\kappa^2\sqrt{\frac{G_o^2}{H_o^2} - 1} + \\ &+ \frac{\epsilon_o}{|a|}\frac{|Z_o|}{\sqrt{Z_o^2 + 4G_o^2}}\int_{\operatorname{arccosh}|G_o/H_o|}^{\operatorname{arccosh}(1/\kappa)} dx\sqrt{1 - \kappa^2\cosh^2 x} - \\ &- \frac{\epsilon_o}{|a|}\frac{Z_o}{\sqrt{Z_o^2 + 4G_o^2}}\int_0^{\operatorname{arccosh}(1/\kappa)} dx\sqrt{1 - \kappa^2\cosh^2 x} \ , \end{aligned} \qquad (82)$$

and

$$\begin{aligned} R &= \frac{\epsilon_o}{|a|}\operatorname{arccosh}\left|\frac{G_o}{H_o}\right| + \frac{\epsilon_o}{|a|}\frac{G_o}{H_o}\kappa^2\sqrt{\frac{G_o^2}{H_o^2} - 1} + \\ &+ \frac{\epsilon_o}{|a|}\frac{|Z_o|}{\sqrt{Z_o^2 + 4G_o^2}}\int_{\operatorname{arccosh}|G_o/H_o|}^{\operatorname{arccosh}(1/\kappa)} dx\sqrt{1 - \kappa^2\cosh^2 x} + \\ &+ \frac{\epsilon_o}{|a|}\frac{Z_o}{\sqrt{Z_o^2 + 4G_o^2}}\int_0^{\operatorname{arccosh}(1/\kappa)} dx\sqrt{1 - \kappa^2\cosh^2 x} \ . \end{aligned} \qquad (83)$$

These results recover those previously obtained in Ref. [20] and Ref. [21]. All quantities $Z_o(s)$, $G_o(s)$, and $H_o(s)$ are functions of the magnetic shear s only.

In the $s << 1$ limit, it can be shown that $Z_o(s) = 1$, $G_o(s) = s\pi/4$, $H_o(s) = -(s\pi/4)(1 + 1/s)\exp(-1/s)$, $T = \epsilon_o s\pi^2/8|a|$ and $R = 2\epsilon_o/|a|s$.[20,24] Equation (81), meanwhile, reduces to Eq. (21) of Ref. [20].

In the $s >> 1$ limit, one finds $Z_o(s) = -(1 - \pi^2/6s - \pi^4/72s^2)$, $G_o(s) = (s\pi/2)$, $H_o(s) = -(s\pi/2)(1 - 1/6s^3)$, $T = \epsilon_o/2s^3\pi^2|a|$ and $R = \epsilon_o\pi^2/15 \cdot 3^{5/2}s^{11/2}|a|$.[23,24]

For arbitrary shear, the functions appearing in Eq. (81) and the tunneling coefficients must be computed numerically. Equation (81) can be rewritten as

$$\frac{\gamma}{|\Omega_o|} = -\frac{|a|^{3/2}}{\epsilon_o^{1/2}}\frac{\hat{\Gamma}(s)}{4\sqrt{2}}\left[\exp\left(-2\frac{\epsilon_o}{|a|}\hat{T}(s)\right) + \exp\left(-2\frac{\epsilon_o}{|a|}\hat{R}(s)\right)\right] , \qquad (84)$$

which is the form proposed by Rosenbluth and coworkers in Ref. [21]. Furthermore, one can readily employ Table 1 for the case $\alpha = 0$ but finite shear. Equation (84) contains the functions $\hat{\Gamma}(s)$, $\hat{T}(s)$ and $\hat{R}(s)$ directly comparable with those of Ref. [21]. The agreement between the results obtained with two completely different techniques[20,21] is reassuring.

B. Finite-Pressure Case

The most important finite pressure ($\alpha \neq 0$) effect on the mode structure involves the mode localization. In particular, as α increases, the WKB turning points are found to shift towards the lower continuous shear Alfvén spectrum. At $\alpha = \alpha_c(s)$, the tunneling region on the lower continuum side disappears; that is $t_T^{(1)} = t_{R(-)}$ and $\theta_{k(-)}^{(0)}(s, \alpha_c) = 0$. The TAE mode then strongly couples to the shear Alfvén continuous spectrum and becomes heavily damped. One can show[24,40] that for $s << 1$

$$\alpha_c \simeq \frac{s^2}{s+1}\left(1 - \left(1 + \frac{1}{s}\right)e^{-1/s}\right) ,$$

and that, for $s >> 1$,

$$\alpha_c \simeq s + 1 - \sqrt{2s+1} \ .$$

It is interesting to note that, for $s >> 1$, α_c asymptotically coincides with the marginal stability of ideal Ballooning modes.[40,41] The values of $\alpha_c(s)$, as obtained from the condition $\theta^{(0)}_{k(-)}(s,\alpha_c) = 0$, are given in Table 2, where they are compared with the analytical predictions. The values of $\alpha_c(s)$ for $s >> 1$ obtained in Ref. [40] from a numerical dispersion relation at $\theta^{(0)}_k = 0$ are slightly higher, since the global threshold coincides with the local result at $\theta^{(0)}_k = \pi$.[23,24]

To examine the damping near $\alpha = \alpha_c(s)$ more carefully, we note that the general expression of the continuum damping rate given by Eq. (78) can be rewritten, with explicit parametric dependences on ϵ_o and $|a|$, as

$$\frac{\gamma}{|\Omega_o|} = -\frac{|a|^{3/2}}{4\sqrt{2\epsilon_o}} \left\{ \hat{\Gamma}_\ell(s,\alpha) \exp\left(-2\frac{\epsilon_o}{|a|}\hat{T}(s,\alpha)\right) + \right.$$
$$\left. + \hat{\Gamma}_u(s,\alpha) \exp\left(-2\frac{\epsilon_o}{|a|}\hat{R}(s,\alpha)\right) \right\} \ , \qquad (85)$$

which reduces to Eq. (84) as $\alpha \to 0$. The definition of the functions $\hat{\Gamma}_\ell(s,\alpha)$, $\hat{T}(s,\alpha)$, $\hat{\Gamma}_u(s,\alpha)$ and $\hat{R}(s,\alpha)$ is evident from a comparison of Eqs. (78) and (85).

Equation (85), however, diverges as $\alpha \to \alpha_c(s)$, since the Taylor expansion of the WKB phase in the expression of the envelope function $A(t)$, as given by Eqs. (74) and (75), as already mentioned, breaks down in this limit. An improved damping can be derived using the leading order WKB radial envelope as it is given by Eqs. (54) and (56).[24] Equation (85) is then modified to

$$\frac{\gamma}{|\Omega_o|} = -\frac{|a|^{3/2}}{4\sqrt{2\epsilon_o}}\left\{W_\ell\,\hat{\Gamma}_\ell(s,\alpha)\,\exp\left(-2\frac{\epsilon_o}{|a|}\hat{T}(s,\alpha)\right) + \right.$$
$$\left. + W_u\,\hat{\Gamma}_u(s,\alpha)\,\exp\left(-2\frac{\epsilon_o}{|a|}\hat{R}(s,\alpha)\right)\right\} \quad . \tag{86}$$

Here, W_ℓ and W_u are weighting factors that approach unity as

$$2\theta^{(0)}_{k(-)}\epsilon_o/|a| >> 1 \ ,$$

(i.e. $n\epsilon_o >> 1$). If we let $\theta^{(0)}_k = \pi - \beta^{(-)}_k\frac{\Omega_o}{|\Omega_o|} + i\eta^{(-)}_k$ in the lower continuum, $\theta^{(0)}_k = \beta^{(+)}_k\frac{\Omega_o}{|\Omega_o|} + i\eta^{(+)}_k$ in the upper continuum, and let $x \equiv |t - t_{R(\pm)}|\cdot|a|/\epsilon_o$, then

$$W_{(u,\ell)}(s,\alpha,\epsilon_o/|a|) = P_{(\pm)}\,\theta^{(0)3/2}_{k(\pm)}\frac{4}{\sqrt{\pi}}\left(\frac{\epsilon_o}{|a|}\right)^{3/2}\int_0^\infty dx\,\sqrt{x^2+2x}\cdot$$
$$\cdot\frac{\exp\left[-2\,(\epsilon_o/|a|)\int_0^x \eta^{(\pm)}_k dx'\right]}{P_{(u,\ell)}\left(x,\beta^{(\pm)}_k,\eta^{(\pm)}_k\right)} \ , \tag{87}$$

with

$$P_{(u,\ell)}\left(x,\beta^{(\pm)}_k,\eta^{(\pm)}_k\right) = \left|\sum_{m=-1}^{\infty} m\,(\pm 1)^m\left\{Z_m\sqrt{x^2+2x}\right.\right.$$
$$\left[\cos\left(m\beta^{(\pm)}_k\right)\sinh\left(m\eta^{(\pm)}_k\right) - i\,\sin\left(m\beta^{(\pm)}_k\right)\cosh\left(m\eta^{(\pm)}_k\right)\right] +$$
$$+\left[\pm 2G_m\,(x+1) + H_{m-1} + H_{m+1} + L_{m+1} - L_{m-1}\right]$$
$$\left.\left.\left[\sin\left(m\beta^{(\pm)}_k\right)\cosh\left(m\eta^{(\pm)}_k\right) + i\,\cos\left(m\beta^{(\pm)}_k\right)\sinh\left(m\eta^{(\pm)}_k\right)\right]\right\}\right| \ .$$

At the continuum position $x = 0$, $\beta^{(\pm)}_k = 0$, $\eta^{(\pm)}_k = \theta^{(0)}_{k(\pm)}$ and $P_{(u,\ell)} = P_{(\pm)}$. In this respect, Eqs. (85) and (86) may be considered as, respectively, the upper and lower bounds for the continuum damping as $\alpha \to \alpha_c(s)$.[24] While the precise determination of the damping in this limit requires a non-perturbative calculation,

we can, however, estimate it. In fact, note that $\hat{T}(s,\alpha_c)=0$, $W_\ell\hat{\Gamma}_\ell(s,\alpha)=O(1-10)$ as $\alpha\rightarrow\alpha_c(s)$ (cf. Table 5 and Ref. [24]) and $\epsilon_o/|a|\equiv(n\epsilon_o)sq_oL_A/r_o$. From Eq. (86) we then have

$$\frac{\gamma}{|\Omega_o|}\simeq 0.18\,\epsilon_o W_\ell\hat{\Gamma}_\ell(s,\alpha)\,(n\epsilon_o)^{-3/2}\,(sq_o)^{-3/2}\left(\frac{r'_o}{L_A}\right)^{3/2}\quad . \tag{88}$$

For the optimal ordering $n\epsilon_o\approx r_o/L_A\approx sq_o=O(1)$, Eq. (88) gives $|\gamma/\epsilon_o\Omega_o|=O(0.1-1)$.

In general, the functions $\hat{\Gamma}_\ell(s,\alpha)$, $\hat{T}(s,\alpha)$, $\hat{\Gamma}_u(s,\alpha)$ and $\hat{R}(s,\alpha)$ appearing in the damping expressions Eqs. (85) and (86), along with the weighting factors W_ℓ and W_u entering in Eq. (86), must be computed numerically and can be conveniently expressed in a tabular form. In the following, results are given for increasing values of α and shear values $s=0.5$ and $s=1.0$ (cf. Tables 3 to 5), which show how the damping increases as α approaches $\alpha_c(s)$. A complete collection of tabulated functions is given in Ref. [24], for $0.1\leq s\leq 3$ and $0\leq\alpha<\alpha_c(s)$.

In the $s<<1,\alpha<<1$ limit, it is possible to give an analytic expression for the functions of the parameters (s,α) entering in the resonant damping expression. With the definitions $\hat{\eta}=(1+1/s)\,e^{-1/s}$ and $\hat{\alpha}=\alpha\,(1+s)/s^2$ the resonant damping of Eq. (85) reduces to[23,24]

$$\begin{aligned}\frac{\gamma}{|\Omega_o|} \;=\; -\frac{|a|^{3/2}}{8\,\pi^{3/2}}\,\frac{1}{s\,\epsilon_o^{1/2}}\left\{\frac{\exp\left[-2\,(\epsilon_o/|a|)\,\hat{T}(s,\alpha)\right]}{\left[(1-\hat{\alpha})^2-\hat{\eta}^2\right]^{1/2}\left[\operatorname{arccosh}\left(\frac{1-\hat{\alpha}}{\hat{\eta}}\right)\right]^{3/2}}+\right.\\ \left.+\;\frac{\exp\left[-2\,(\epsilon_o/|a|)\,\hat{R}(s,\alpha)\right]}{\left[(1+\hat{\alpha})^2-\hat{\eta}^2\right]^{1/2}\left[\operatorname{arccosh}\left(\frac{1+\hat{\alpha}}{\hat{\eta}}\right)\right]^{3/2}}\right\}\quad,\end{aligned} \tag{89}$$

with

$$\hat{T}(s,\alpha)\;\simeq\;\frac{s^2\pi^2}{8}\operatorname{arccosh}\left(\frac{1-\hat{\alpha}}{\hat{\eta}}\right)\left[(1-\hat{\alpha})^2+\frac{\hat{\eta}^2}{2}\right]\quad,$$

$$\hat{R}(s,\alpha) \simeq 2\,\mathrm{arccosh}\left(\frac{\hat{\alpha}}{\hat{\eta}} + \frac{2}{s\pi\hat{\eta}}\right) .$$

VIII. Summary and Discussions

In the present work, we have formulated a general theoretical approach for analyzing the two-dimensional structure of high-n Toroidal Alfvén Eigenmodes in large-aspect-ratio tokamaks, using the well known (s, α) equilibrium model.[28] Such studies determine the radial envelope of the poloidal harmonics and, thus, are important in assessing the resonant damping rate due to finite coupling to the continuous shear Alfvén spectrum.

The present approach naturally treats modes with extended radial structures characterized by well-spaced WKB turning point pairs (cf. Fig.4), and is also capable of analyzing the finite coupling between two-dimensional high-n discrete and continuous spectra as well as other non-ideal effects.[36] In this respect, it may be regarded as a generalized ballooning formalism. The technique employed here to "generate" a radial eigenvalue problem from the local dispersion relation (see the discussion given in Section II) is, meanwhile, very general, and can be used for the solution of any two-dimensional problem characterized by two distinct scales, e.g. typically for high-n modes.[37]

In this work, we have further specialized our considerations to the case of linearly varying equilibrium profiles in order to illustrate the application of this formalism in sufficient details. In the $\alpha = 0$ pressureless limit, the previously obtained results[20,21] are recovered. The analysis has also been generalized to the case with arbitrary shear s and dimensionless pressure gradient α. In particular, it is demonstrated that a critical value $\alpha_c(s)$ exists (which asymptotically coincides with the Troyon limit), at which the tunneling region of the TAE radial envelope towards the lower shear Alfvén continuum disappears, causing a strong coupling of the mode to the con-

tinuous spectrum. The corresponding resonant damping rate, meanwhile, increases significantly as $\alpha_c(s)$ is approached and is typically ordered as $O(0.1-1)\epsilon_o\omega_A$.

The damping given by Eqs. (78) and (86) must be compared with, e.g., the electron Landau damping $(\gamma/|\Omega_o|)_L \approx -(\beta_e m_e/m_i)^{1/2}$. In ITER,[42] for example, the toroidal magnetic field on axis is $\approx 5T$, the electron density is $n_e \lesssim 10^{14} cm^{-3}$ and the peak electron temperature is $T_e \approx 35KeV$. Thus $\beta_e \approx 0.05$ and $(\gamma/|\Omega_o|)_L \approx -3.7\text{x}10^{-3}$. In the case of TFTR and JET, the electron Landau damping is even lower, because of the lower $T_e \approx 5KeV$. To get an estimate of the continuum damping, we need to give an order of magnitude for α and s in these devices. Since the resonant excitation of TAE's occurs close to the plasma center, where most of the fusion alphas are born, s is expected to be small due to the relatively flat $q(r)$ profile. Similarly, estimating $\alpha \approx< \beta > R_o/a$, we have $\alpha \gtrsim 0.15$ in ITER, while $\alpha \approx 0.03-0.05$ in TFTR and JET. Taking a common value of $s = 0.5$ for all these machines, we see that ITER would be above the predicted $\alpha_c \simeq 0.14$ threshold for strong continuum TAE damping. Taking $\epsilon_o = 0.2-0.3$, $n\epsilon_o \approx 1$ (i.e. $n = 3-5$), $|a| \approx 1/n$ and $s = 0.5$, with the help of Tables 3 and 5, we have $(\gamma/|\Omega_o|)_r \approx -(1-1.5)\text{x}10^{-2}$ for $\alpha = 0.05$ and $(\gamma/|\Omega_o|)_r \approx -(3-5)\text{x}10^{-2}$ for $\alpha = 0.13$, the subscript r staying for 'resonant damping'. In both cases, the continuum (resonant) damping is much larger (an order 5 to 20) than the electron Landau damping. Close to $\alpha_c \simeq 0.14$ the damping is already of order $O(\epsilon_o)$ as expected for $\alpha \gtrsim \alpha_c$. In the presence of circulating beam particles (or fusion alphas), the linear mode drive is $(\gamma/|\Omega_o|) \simeq \beta_h f_h k_\vartheta \rho_h R_o/L_{Ph}$,[11] with ρ_h being the Larmor radius of the energetic ('hot', subscript h) particles, L_{Ph} the scale length of their pressure profile, f_h the fraction of resonant particles, and $k_\vartheta \rho_h \approx \epsilon_o/s$.[11,16] Thus,

assuming $\epsilon_o R_o/L_{Ph} \approx f_h \approx O(1)$, we have a marginal stability threshold for TAE modes at $\beta_h \approx O(|\gamma/|\Omega_o||_r) = O(10^{-2}, 10^{-1})$,[20,23] the higher values corresponding to $\alpha \gtrsim \alpha_c$. This values are of the same order of the ones discussed in Ref. [43], but they are a consequence of the global equilibrium properties of hot plasmas, and not of a finite plasma conductivity. Looking at the values of $(\gamma/|\Omega_o|)_r$ obtained previously, we can conclude that TAE might be difficult to excite close to the threshold $\alpha = \alpha_c$. It is necessary to remark that our theoretical results only give approximated estimates of the continuum damping for $n\epsilon_o \approx 1$; appropriate for the present experiments. We can, nevertheless, conclude that finite pressure effects will be very important in enhancing the TAE continuum damping, especially in the central, low shear, plasma region, where α_c could be easily exceeded. This stabilizing effect should be more significant in ITER, where α is larger and medium to high toroidal mode numbers can be excited. In the present machines, such as TFTR and JET, $n \lesssim 3$ are more likely dominant and the finite-α continuum damping enhancement has to be taken as a qualitative indication, since the damping rates of low-n TAE's, in principle, must be computed numerically.

One interesting feature of the high-n TAE eigenmode structure is the short poloidal wavelength of order $O(a/m_o)$ and the rather broad extent of the radial envelope; i.e. $O(\epsilon_o L_A)$ and $O(\epsilon_o^{1/4} r_o (L_A/nr_o)^{1/2})$ in the cases of, respectively, linear and parabolic radial equilibrium profiles. These broad radial structures suggest that, at least in the linear phase, the plasma may develop vortices with long radial correlation length, and, therefore, may have significant implications to transport issues.[37,38]

Finally we note that, while we have limited our present work to a model equi-

librium with shifted circular magnetic surfaces, the theoretical approach developed here could be straightforwardly extended to equilibria with finite ellipticity and triangularity. In such cases there are additional modes, such as high-n Ellipticity induced Alfvén Eigenmodes[44] etc.. On the other hand, the physical picture of continuum damping, as developed here, can be expected to remain about the same.

The present formalism could be also further generalized to include effects such as equilibria with flow as well as wave-particle resonances to have a more complete description of instability damping and growth mechanisms.

Acknowledgments

This work was supported by U.S. Department of Energy Contract No. DE-AC02-76-CHO-3073.

Appendix A. Singular Structure of the Resonant Poloidal Harmonics

Let us consider Eqs. (34) of Section III. We will focus our attention on a case in which the resonance involves the ℓ and the $\ell+1$ poloidal harmonics, i.e., we will find the behaviour of these solutions, close to the point where the cylindrical continuous shear Alfvén spectra of the ℓ and $\ell+1$ modes coalesce. This occurs for $t \simeq \ell + 1/2$. Let $x \equiv (t-\ell)$. Then we have the Euler-Lagrange equations

$$
\begin{aligned}
& s^2 \frac{\partial}{\partial x}\left[(x+1)^2 - \Omega_o^2\right] \frac{\partial}{\partial x}\delta\phi_{\ell-1} - \epsilon_o \Omega_o^2 s^2 \frac{\partial^2}{\partial x^2}\left(\delta\phi_{\ell-2} + \delta\phi_\ell\right) + \ldots = 0 \ , \\
& s^2 \frac{\partial}{\partial x}\left[x^2 - \Omega_o^2\right] \frac{\partial}{\partial x}\delta\phi_{\ell} - \epsilon_o \Omega_o^2 s^2 \frac{\partial^2}{\partial x^2}\left(\delta\phi_{\ell-1} + \delta\phi_{\ell+1}\right) + \ldots = 0 \ , \qquad \text{(A.1)} \\
& s^2 \frac{\partial}{\partial x}\left[(x-1)^2 - \Omega_o^2\right] \frac{\partial}{\partial x}\delta\phi_{\ell+1} - \epsilon_o \Omega_o^2 s^2 \frac{\partial^2}{\partial x^2}\left(\delta\phi_{\ell} + \delta\phi_{\ell+2}\right) + \ldots = 0 \ .
\end{aligned}
$$

Here, only the highest order radial derivatives appearing in Eqs. (34) have been included explicitly. The dots stay for the remaining terms, which are negligible in the present analysis. Since $\Omega_o^2 \simeq 1/4$ and $x \simeq 1/2$, only $[x^2 - \Omega_o^2]$ and $[(x-1)^2 - \Omega_o^2]$ are vanishing in the region of interest. Assume $\Omega_o \simeq 1/2$ (the case $\Omega_o \simeq -1/2$ is identically equivalent). Then, given $\delta\Omega_o \equiv \Omega_o - 1/2$ and $\delta x \equiv x - 1/2$, we have

$$
\begin{aligned}
[x^2 - \Omega_o^2] &\simeq \delta x - \delta\Omega_o \ , \\
[(x-1)^2 - \Omega_o^2] &\simeq -\delta x - \delta\Omega_o \ .
\end{aligned}
$$

Equations (A.1) can be treated with a two scale analysis, given the slow scale x and the fast scale $y \equiv \delta x/\epsilon_o\Omega_o^2$. To do so, we expand $\delta\phi_j$ as

$$
\delta\phi_i = \delta\phi_j^{(0)}(x,y) + \epsilon_o\Omega_o^2\delta\phi_j^{(1)}(x,y) + \ldots \ .
$$

To the lowest order, the first of Eqs. (A.1) is then

$$s^2\left[(x+1)^2-\Omega_o^2\right]\frac{\partial^2}{\partial y^2}\frac{1}{\epsilon_o\Omega_o^2}\delta\phi_{\ell-1}^{(0)} = 0 \ ,$$

from which

$$\delta\phi_{\ell-1}^{(0)}(x,y) = \delta\phi_{\ell-1}^{(0)}(x) + yF(x) \ ,$$

where $F(x)$ must be set to zero in order to avoid secularities in the fast variable y. Therefore, $\delta\phi_{\ell-1}$ does not have any structure on the fast scale y to the lowest order. The singular behaviour appears in the next order, driven by the harmonic $\delta\phi_\ell^{(0)}$; i.e.,

$$s^2\left[(x+1)^2-\Omega_o^2\right]\frac{\partial^2}{\partial y^2}\delta\phi_{\ell-1}^{(1)} = s^2\,\frac{\partial^2}{\partial y^2}\delta\phi_\ell^{(0)} \ ,$$

but the determination of the first order correction is beyond our need. The same calculation could be done for $\delta\phi_{\ell+2}$, which in general proves how, close to a given resonance, only the two closest neighbouring harmonics (in this case $\delta\phi_\ell$ and $\delta\phi_{\ell+1}$) exhibit a singular behaviour to the lowest order in the expansion parameter $\epsilon_o\Omega_o^2$.

Therefore, to the lowest order, Eqs. (A.1) reduce to

$$\begin{aligned} s^2\,\frac{\partial}{\partial y}\left[y-\frac{\delta\Omega_o}{\epsilon_o\Omega_o^2}\right]\frac{\partial}{\partial y}\delta\phi_\ell^{(0)} - s^2\,\frac{\partial^2}{\partial y^2}\delta\phi_{\ell+1}^{(0)} &= 0 \ , \\ s^2\,\frac{\partial}{\partial y}\left[y+\frac{\delta\Omega_o}{\epsilon_o\Omega_o^2}\right]\frac{\partial}{\partial y}\delta\phi_{\ell+1}^{(0)} + s^2\,\frac{\partial^2}{\partial y^2}\delta\phi_\ell^{(0)} &= 0 \ . \end{aligned} \qquad \text{(A.2)}$$

These equations are equivalent to the system

$$\begin{aligned} s^2\frac{\partial}{\partial x}\left[x^2-\Omega_o^2\right]\frac{\partial}{\partial x}\delta\phi_\ell^{(0)} - \epsilon_o\Omega_o^2 s^2\frac{\partial^2}{\partial x^2}\delta\phi_{\ell+1}^{(0)} &= 0 \ , \\ s^2\frac{\partial}{\partial x}\left[(x-1)^2-\Omega_o^2\right]\frac{\partial}{\partial x}\delta\phi_{\ell+1}^{(0)} - \epsilon_o\Omega_o^2 s^2\frac{\partial^2}{\partial x^2}\delta\phi_\ell^{(0)} &= 0 \ . \end{aligned} \qquad \text{(A.3)}$$

solved as $x \to 1/2$. Equations (A.3) are exactly integrable, and give

$$\frac{\partial}{\partial x}\delta\phi_\ell^{(0)} = \frac{B_\ell\left((x-1)^2-\Omega_o^2\right)+\epsilon_o\Omega_o^2 C_\ell}{D_\ell}\ , \tag{A.4}$$

$$\frac{\partial}{\partial x}\delta\phi_{\ell+1}^{(0)} = \frac{C_\ell\left(x^2-\Omega_o^2\right)+\epsilon_o\Omega_o^2 B_\ell}{D_\ell}\ , \tag{A.5}$$

$$D_\ell = \left(x^2-\Omega_o^2\right)\left((x-1)^2-\Omega_o^2\right)-\epsilon_o^2\Omega_o^4\ , \tag{A.6}$$

where B_ℓ and C_ℓ are integration constants.

The coefficients B_ℓ and C_ℓ can be expressed in terms of the regular part of the magnetic field compression at resonance, $\widehat{\delta B}_{\|,\ell}$ and $\widehat{\delta B}_{\|,\ell+1}$. More precisely, we have that[24]

$$\begin{aligned} B_\ell &= -\frac{\omega}{c}q_o^2R_o^2\frac{\widehat{\delta B}_{\|,\ell}}{s}\ , \\ C_\ell &= -\frac{\omega}{c}q_o^2R_o^2\frac{\widehat{\delta B}_{\|,\ell+1}}{s}\ . \end{aligned} \tag{A.7}$$

Equations (A.7) along with Eq. (63) demonstrate that the wave absorption at the resonance with the shear Alfvén continuous spectrum is proportional to the amplitude square of the magnetic field compression, as already emphasized by Chen and Hasegawa[45] for the cylindrical case.

Appendix B. Fourier Transform of the Ballooning Eigenfunction

From Eq. (36), we know that in order to determine the functional form of the poloidal harmonics $\delta\phi_j(t)$, we need to calculate

$$\phi(t, t-j) = \phi(t,x) = \int_{-\infty}^{+\infty} d\theta\, e^{-ix\theta}\, \Phi(t,\theta) \ .$$

Recall that $\Phi(t,\theta) = \delta\psi\,[1+I_o^2]^{-1/2}$ (cf. Section IV.A); thus,

$$\phi(t,x) = \int_{-\infty}^{+\infty} \frac{d\theta}{\sqrt{1+I_o^2}}\, \delta\psi(t,\theta)\, e^{-i\theta x} \ . \tag{B.1}$$

According to Eqs. (A.4) and (A.5) of Appendix A, we need to determine $\partial_t \delta\phi_j(t)$ close to a given 'resonance'; i.e., for $|t-j\pm 1/2| < \epsilon_o$. Since the envelope function $A(t)$ is slowly varying, we have

$$\partial_t \delta\phi_j(t) = A(j)\,\partial_x \phi(j,x) \simeq A(t)\,\partial_x\phi(t,x) \ .$$

Thus we are left with the calculation of

$$e^{ix\theta_k^{(0)}}\,\frac{\partial}{\partial x}\,\phi(t,x) = -i\int_{-\infty}^{+\infty} d\theta\,\frac{\theta}{\sqrt{1+I_o^2}}\,\delta\psi(t,\theta)\,e^{-ix(\theta-\theta_k^{(0)})} \ .$$

Now, as in Section IV.A, let us introduce the scale T, such that $|sT| >> \mathrm{Max}(1,\alpha)$ and $|\epsilon_o T| << 1$. Similarly, we will also use the shifted variable $\theta' = \theta - \theta_k^{(0)}$, and, then, omit the prime superscript. The contribution to $\partial_x\phi(t,x)$, thus, comes from two distinct regions: $|\theta| < T$ (Internal Region), and $|\theta| > T$ (External Region); that is,

$$
\begin{aligned}
e^{i x \theta_k^{(0)}} \frac{\partial}{\partial x} \phi(t,x) \;=\; & -i \int_0^T d\theta \, \frac{\theta + \theta_k^{(0)}}{\sqrt{1 + \left[s\theta - \alpha \sin\left(\theta + \theta_k^{(0)}\right)\right]^2}} \, \delta\psi_I^{(+)}(t,\theta)\, e^{-ix\theta} \; - \\
& -i \int_0^T d\theta \, \frac{\theta - \theta_k^{(0)}}{\sqrt{1 + \left[s\theta - \alpha \sin\left(\theta - \theta_k^{(0)}\right)\right]^2}} \, \delta\psi_I^{(-)}(t,-\theta)\, e^{ix\theta} \; - \\
& -\frac{i}{s} \int_T^\infty d\theta \left[\delta\psi_E^{(+)}(t,\theta)\, e^{-ix\theta} \; - \; \delta\psi_E^{(-)}(t,-\theta)\, e^{ix\theta} \right] \; + \\
& + O\left(\frac{1}{T}\right) + O\left(\frac{1}{s^2T^2}\right) + O\left(\frac{\alpha}{sT}\right) \; ;
\end{aligned}
$$

where the $(\pm)$ superscript refers to solutions $\delta\psi$ for positive and negative arguments, respectively. The contribution from the integral of the External Region is typically of order $O(1/\epsilon_o)$ for $|x \pm 1/2| = O(\epsilon_o)$, while the contribution from the Internal Region is of order $O(T)$. Thus

$$
\begin{aligned}
e^{i x \theta_k^{(0)}} \frac{\partial}{\partial x} \phi(t,x) \;=\; & -\frac{i}{s} \int_T^\infty d\theta \left[\delta\psi_E^{(+)}(t,\theta)\, e^{-ix\theta} \; - \; \delta\psi_E^{(-)}(t,-\theta)\, e^{ix\theta} \right] \\
& + O\left(\frac{1}{T}\right) + O\left(\frac{1}{s^2T^2}\right) + O\left(\frac{\alpha}{sT}\right) + O(\epsilon_o T) \; .
\end{aligned}
$$

In the External Region, the solution $\delta\psi_E^{(\pm)}$ is given by Eq. (45). Thus, defining $\Delta_{(\pm)} = (a^{(+)} \pm a^{(-)})$, we have

$$
\frac{\partial}{\partial x} \phi(t,x) \;=\; -\frac{i}{2s} \left(\Delta_{(+)}\, I_1 \; + \; \Delta_{(-)}\, I_2 \right) e^{-i x \theta_k^{(0)}} \; , \tag{B.2}
$$

with

$$
\begin{aligned}
I_{1,2} \;=\; \int_T^\infty d\theta \, e^{-\hat{\gamma}\theta} \left\{ \sqrt{-\Gamma_-} \left[\cos\left(\frac{\theta + \theta_k^{(0)}}{2}\right) e^{-ix\theta} \; \mp \; \cos\left(\frac{\theta - \theta_k^{(0)}}{2}\right) e^{ix\theta} \right] \; + \right. \\
\left. + \sqrt{\Gamma_+} \left[\sin\left(\frac{\theta + \theta_k^{(0)}}{2}\right) e^{-ix\theta} \; \mp \; \sin\left(\frac{\theta - \theta_k^{(0)}}{2}\right) e^{ix\theta} \right] \right\} \; ,
\end{aligned}
$$

where the upper sign refers to I_1, and the lower sign to I_2. From these expressions, we can show that

$$I_1 = e^{i\theta_k^{(0)}/2}\, i\,\Im\left[\left(\sqrt{-\Gamma_-} - i\sqrt{\Gamma_+}\right) e^{-\hat{\gamma}T}\, \frac{e^{-iT(x-1/2)}}{\hat{\gamma} + i(x-1/2)}\right] + \\ + e^{-i\theta_k^{(0)}/2}\, i\,\Im\left[\left(\sqrt{-\Gamma_-} + i\sqrt{\Gamma_+}\right) e^{-\hat{\gamma}T}\, \frac{e^{-iT(x+1/2)}}{\hat{\gamma} + i(x+1/2)}\right] ,$$

$$I_2 = e^{i\theta_k^{(0)}/2}\, \Re\left[\left(\sqrt{-\Gamma_-} - i\sqrt{\Gamma_+}\right) e^{-\hat{\gamma}T}\, \frac{e^{-iT(x-1/2)}}{\hat{\gamma} + i(x-1/2)}\right] + \\ + e^{-i\theta_k^{(0)}/2}\, \Re\left[\left(\sqrt{-\Gamma_-} + i\sqrt{\Gamma_+}\right) e^{-\hat{\gamma}T}\, \frac{e^{-iT(x+1/2)}}{\hat{\gamma} + i(x+1/2)}\right] .$$

Noting that $\partial_t\, \delta\phi_j \simeq A(t)\, \partial_x\, \phi(t,x)$ and Eq. (B.2), we have, for $|x \mp 1/2| = O(\epsilon_o)$,

$$N(t)\, s\, \frac{\partial}{\partial x}\, \delta\phi_j = \frac{e^{\pm i\theta_k^{(0)}/2} A(j)}{\hat{\gamma}^2 + (x \mp 1/2)^2} \left[\mp\hat{\gamma}\left(\sqrt{\Gamma_+}\, \frac{N(t)\,\Delta_{(+)}}{2} \pm i\sqrt{-\Gamma_-}\, \frac{N(t)\,\Delta_{(-)}}{2}\right)\right. \\ \left. - \left(x \mp \frac{1}{2}\right)\left(\sqrt{-\Gamma_-}\, \frac{N(t)\,\Delta_{(+)}}{2} \mp i\sqrt{\Gamma_+}\, \frac{N(t)\,\Delta_{(-)}}{2}\right)\right] . \quad \text{(B.3)}$$

Here, $N(t)$ is the normalization factor introduced in Section V. From the matching of Eqs. (50) and (51), we find that $\Delta_{(\pm)}$ are given by

$$\frac{N(t)\,\Delta_{(\pm)}}{2} = \pm\cos\left(\frac{\theta_k^{(0)}}{2}\right)\left[\sqrt{-\Gamma_-}\, \frac{\delta\psi_c \pm \delta\bar{\psi}_c}{2} + \sqrt{\Gamma_+}\, \frac{\delta\psi_s \pm \delta\bar{\psi}_s}{2}\right] \mp \\ \mp \sin\left(\frac{\theta_k^{(0)}}{2}\right)\left[\sqrt{-\Gamma_-}\, \frac{\delta\psi_s \mp \delta\bar{\psi}_s}{2} - \sqrt{\Gamma_+}\, \frac{\delta\psi_c \mp \delta\bar{\psi}_c}{2}\right] .$$

Now, considering that $A_{j\pm1} = e^{\pm i\theta_k} A_j$ in the decaying region (i.e., also for the resonant poloidal harmonics), we finally have, for $|x - 1/2| = O(\epsilon_o)$,

$$N(t)\, s\, \frac{\partial}{\partial x}\delta\phi_j = \frac{1}{\hat{\gamma}^2 + (x-1/2)^2}\left\{ -\hat{\gamma}\left[\left(\hat{\gamma}\hat{a}_- + (\Omega_o^2 - 1/4)\hat{b}_+\right) A_j + \right.\right.$$
$$+ \epsilon_o \Omega_o^2 \hat{b}_- A_{j+1}\,] - (x-1/2)\left[\left(\hat{\gamma}\hat{b}_+ - .(\Omega_o^2 - 1/4)\hat{a}_-\right) A_j + \right.$$
$$\left.\left. + \epsilon_o\, \Omega_o^2 \hat{a}_+ A_{j+1}\,]\right\}\ , \qquad \text{(B.4)}$$

$$N(t)\, s\, \frac{\partial}{\partial x}\delta\phi_{j+1} = \frac{1}{\hat{\gamma}^2 + (x-1/2)^2}\left\{ \hat{\gamma}\left[\left(\hat{\gamma}\hat{a}_+ + (\Omega_o^2 - 1/4)\hat{b}_-\right) A_{j+1} + \right.\right.$$
$$+ \epsilon_o \Omega_o^2 \hat{b}_+ A_j\,] - (x-1/2)\left[\left(\hat{\gamma}\hat{b}_- - (\Omega_o^2 - 1/4)\hat{a}_+\right) A_{j+1} + \right.$$
$$\left.\left. + \epsilon_o\, \Omega_o^2 \hat{a}_- A_j\,]\right\}\ , \qquad \text{(B.5)}$$

with

$$\hat{a}_\pm = \frac{\delta\psi_c + \delta\bar{\psi}_c}{2} \pm i\,\frac{\delta\psi_s - \delta\bar{\psi}_s}{2}\ ,$$
$$\hat{b}_\pm = \frac{\delta\psi_s + \delta\bar{\psi}_s}{2} \pm i\,\frac{\delta\psi_c - \delta\bar{\psi}_c}{2}\ . \qquad \text{(B.6)}$$

Equations (B.4) and (B.5) must match the corresponding expressions obtained by direct solution of the two-mode truncated Eq. (34) of Section III (see Appendix A); i.e.,

$$\frac{\partial}{\partial x}\delta\phi_j = \frac{B_j\,((x-1)^2 - \Omega_o^2) + \epsilon_o\Omega_o^2\, C_j}{D_j}\ , \qquad (A.4)$$

$$\frac{\partial}{\partial x}\delta\phi_{j+1} = \frac{C_j\,(x^2 - \Omega_o^2) + \epsilon_o\Omega_o^2\, B_j}{D_j}\ , \qquad (A.5)$$

$$D_j = \left(x^2 - \Omega_o^2\right)\left((x-1)^2 - \Omega_o^2\right) - \epsilon_o^2\Omega_o^4\ . \qquad (A.6)$$

For $|x - 1/2| = O(\epsilon_o)$ and $|\Omega_o^2 - 1/4| = O(\epsilon_o)$, we have

$$D_j = -\left((x-1/2)^2 + \hat{\gamma}^2\right)\ .$$

Thus, we finally obtain

$$
\begin{aligned}
N(j+1/2)\,s\,B_j &= -\left(\hat{\gamma}\hat{b}_+ - (\Omega_o^2 - 1/4)\hat{a}_-\right) A_j - \epsilon_o \Omega_o^2 \hat{a}_+ A_{j+1} \ , \\
N(j+1/2)\,s\,C_j &= \left(\hat{\gamma}\hat{b}_- - (\Omega_o^2 - 1/4)\hat{a}_+\right) A_{j+1} + \epsilon_o \Omega_o^2 \hat{a}_- A_j \ . \qquad \text{(B.7)}
\end{aligned}
$$

The amplitudes A_j are themselves proportional to the normalization function $N(t)$,[24] since $|A(t)|^2 \approx (\partial F/\partial \theta_k^{(0)})^{-1} \approx |N(t)|^2$. This makes the coefficients B_j and C_j, defined in Eqs. (B.7), independent on $N(t)$.

References

[1]A.B. Mikhailovskii, Zh. Eksp. Teor. Fiz. **68**, 1772 (1975) [Sov. Phys. JETP **41**, 890 (1975)].

[2]M.N. Rosenbluth and P.H. Rutherford, Phys. Rev. Lett. **34**, 1428 (1975).

[3]K.T. Tsang, D.J. Sigmar, J.C. Whitson, Phys. Fluids **24**, 1508 (1981).

[4]H. Grad, Phys. Today **22**, 34, (1969).

[5]C.E. Kieras and J.A. Tataronis, J. Plasma Physics **28**, 395, (1982).

[6]C.Z. Cheng, Liu Chen, M.S. Chance, Annals of Physics, vol. 161, 21, Apr. 1985.

[7]C.Z. Cheng and M.S. Chance, Phys. Fluids, **29**, 3695, (1986).

[8]D.J. Sigmar, C.T. Hsu, R. White, and C.Z. Cheng, Phys. Fluids B, **4**, 1492 and 1506, (1992).

[9]K.L. Wong et al., Phys. Rev. Lett. **66**, 1874, (1991).

[10]W.W. Heidbrink, E.J. Strait, E. Doyle, and R. Snider, Nucl. Fusion **31**, 1635 (1991).

[11]Liu Chen, in Theory of Fusion Plasmas, Ed. J. Vaclavik, F. Troyon, and E. Sindoni (Editrice Compositori, Bologna, 1989), p. 327.
C.Z. Cheng, G.Y. Fu, and J.W. Van Dam, *ibid.*, p.259.

[12]Liu Chen et al., in Proc. 12th Intl. Conf. on Plasma Physics and Controlled Nucl. Fusion Research (Nice, France), vol. 2, p.77, IAEA, Vienna 1989.

[13]G.Y. Fu and J.W. Van Dam, Phys. Fluids B, **1**, 1949, (1989).

[14]R. Betti and J.P. Freidberg, Phys. Fluids B **4**, 1465, (1992).

[15]H.L. Berk, B.N. Breizman, and H. Ye, Phys. Lett. A **162**, 475 (1992).

[16]H. Biglari, F. Zonca, and L. Chen, Phys. Fluids B **4**, 2385 (1992).

[17]G.Y. Fu and C.Z. Cheng, Princeton Plasma Physics Laboratory, Report PPPL-2852, (1992).

[18]A.B. Mikhailovskii and I.G. Shuchman, Zh. Eksp. Teor. Fiz. **71**, 1813 (1976).

[19]N.N. Gorelenkov and S.E. Sharapov, Phys. Scr. **45**, 163, (1992).

[20]F. Zonca and L. Chen, Phys. Rev. Lett., **68**, 592, (1992).

[21]M.N. Rosenbluth, H.L. Berk, J.W. Van Dam, and D.M. Lindberg, Phys. Rev. Lett., **68**, 596, (1992).

[22]H.L. Berk, J.W. Van Dam, Z. Guo, and D.M. Lindberg, Phys. Fluids B, **4**, 1806, (1992).

[23]F. Zonca and L. Chen, in: Proc. Int. Sherwood Fusion Conference, Seattle, WA (1991); and Bull. Am. Phys. Soc. **33**, 2395, (1991).

[24]Fulvio Zonca, Ph.D. Thesis, Princeton University, Plasma Physics Laboratory, Princeton (Jan. 1993).

[25]J.W. Connor, R.J. Hastie, and J.B. Taylor, Proc. R. Soc. London Ser. A, **365**, 1, (1979).

[26]R.L. Dewar, J. Manickam, R.C. Grimm, M.S. Chance, Nucl. Fusion **21**, 493, (1981).

[27]Y.C. Lee and J.W. Van Dam, in Proceedings of the Finite-Beta Theory Workshop, Varenna 1977, edited by B. Coppi and W. Sadowski, U.S. D.o.E., CONF-7709 167, p.93, (1977).

[28]C.M. Bishop, CLM-R249, Culham (1985).

[29]J.W. Connor and R.J. Hastie, CLM-M-106, Culham (1985).

[30]F. Troyon, R. Gruber, H. Saurenmann, S. Semenzato, and S. Succi, Plasma Physics **26**, 209, (1984).

[31]E. Gerjuoy, A.R.P. Rau, and L. Spruch, Rev. Mod. Phys. **55**, 725, (1983).

[32]H. Goldstein, "Classical Mechanics", Addison-Wesley (1980).

[33]I.B. Bernstein and L. Friedland, in Basic Plasma Physics, vol. I, pp. 367-418, A.A. Galeev and R.N. Sudan Editors, Amsterdam (1983).

[34]D. Choi and W. Horton, Phys. Fluids **23**, 356, (1980).

[35]R.J. Hastie, K.W. Hesketh, and J.B. Taylor, Nucl. Fusion **19**, 1223, (1979).

[36]E.A. Frieman, G. Rewoldt, W.M. Tang, and A.H. Glasser, Phys. Fluids **23**, 1750, (1980).

[37]F. Romanelli and F. Zonca, submitted to Phys. Fluids B (1993).

[38]J.W. Connor, J.B. Taylor, and H.R. Wilson, AEA FUS 197, Culham (1992).

[39]A. Parmeggiani, private communication.

[40]G.Y. Fu and C.Z. Cheng, Phys. Fluids B, **2**, 985, (1990).

[41]L. Chen, A. Bondeson and M.S. Chance, Nuclear Fusion **27**, 1918, (1987).

[42]K. Tamabechi, J.R. Gilleland, Yu. A. Sokolov, R. Toschi and ITER Team, Nucl. Fusion, **31**, 1135, (1991).

[43]R.R. Mett and S.M. Mahajan, Phys. Fluids B **4**, 2885, (1992).

[44]R. Betti and J.P. Freiberg, Phys. Fluids B, **3**, (1991).

[45]A. Hasegawa and L. Chen, Phys. Rev. Lett. **32**, 454, (1974); and L. Chen and A. Hasegawa Phys. Fluids **17**, 1399, (1974).

Table Captions

Table 1: Coefficients $Z_o(s)$, $G_o(s)$ and $H_o(s)$ of the local dispersion relation, and $\hat{\Gamma}(s)$, $\hat{T}(s)$ and $\hat{R}(s)$ appearing in the damping expression Eq. (84), as a function of the magnetic shear s.

Table 2: Values of $\alpha_c(s)$ from $\theta^{(0)}_{k(-)}(s, \alpha_c(s)) = 0$, compared with the asymptotic limits, $s << 1$ and $s >> 1$, computed analytically.

Table 3: Values of the functions $\hat{\Gamma}_u(s,\alpha)$, $\hat{R}(s,\alpha)$, $\hat{\Gamma}_\ell(s,\alpha)$ and $\hat{T}(s,\alpha)$ versus α at $s = 0.5$.

Table 4: Values of the functions $\hat{\Gamma}_u(s,\alpha)$, $\hat{R}(s,\alpha)$, $\hat{\Gamma}_\ell(s,\alpha)$ and $\hat{T}(s,\alpha)$ versus α at $s = 1.0$.

Table 5: Values of the functions $W_\ell \hat{\Gamma}_\ell(s,\alpha)$ and $W_u \hat{\Gamma}_u(s,\alpha)$ versus α at $s = 0.5$ and $s = 1.0$. The asymptotic parameter is $\epsilon_o/|a| = 100$ in this case.

Figure Captions

Figure 1: Continuous spectra for the (m, n) (full circles) and $(m+1, n)$ (crosses) cylindrical shear Alfvén modes. When toroidicity effects are included, a frequency gap appears in the shear Alfvén continuum. Here nq has been used as a radial variable.

Figure 2: (a) Gap formation and gap structure for the poloidal harmonics m, $m+1$ and $m+2$. The form of each eigenfunction is given; in (b) for $\delta\phi_m$, in (c) for $\delta\phi_{m+1}$ and in (d) for $\delta\phi_{m+2}$.

Figure 3: (a) TAE eigenmode structure. The gap region $|n\Delta q| \approx n\epsilon_o|q'L_A|$ corresponds to the spatial interval in which the TAE frequency is in the forbidden frequency window of the continuous spectrum. The amplitude of the poloidal harmonics outside the TAE localization region is exponentially small. Here $\delta\phi = \sum_m \delta\phi_m \exp(-im\theta)$. (b) Resonant excitation of the shear Alfvén continuum at the TAE frequency.

Figure 4: Relation between the radial profile of the dispersion function $F(\theta_k^{(0)}, \Omega_o^2, \alpha, s)$ and the real WKB phase trajectories in the $(\theta_k^{(0)}, t)$ plane. Ω_o labels different phase trajectories. The structure repeats in $\theta_k^{(0)}$ with period 2π, $\theta_k^{(0)}$ being a polidromic function of t.

Figure 5: The shaded area is quantized according to the global dispersion relation of TAE modes, Eq. (57).

Table 1:

s	$Z_0(s)$	$G_0(s)$	$H_0(s)$	$\hat{\Gamma}(s)$	$\hat{T}(s)$	$\hat{R}(s)$
0.1	0.98754E+00	0.78680E-01	-0.57015E-04	0.56840E-01	0.80080E-01	0.18775E+02
0.2	0.94836E+00	0.15889E+00	-0.97539E-02	0.96756E-01	0.10422E+00	0.83021E+01
0.3	0.87971E+00	0.24481E+00	-0.58349E-01	0.13661E+00	0.95112E-01	0.45152E+01
0.4	0.78743E+00	0.34239E+00	-0.14914E+00	0.18102E+00	0.76062E-01	0.24668E+01
0.5	0.68356E+00	0.45388E+00	-0.26984E+00	0.23368E+00	0.58440E-01	0.12704E+01
0.6	0.57799E+00	0.57804E+00	-0.40945E+00	0.29666E+00	0.44723E-01	0.62503E+00
0.7	0.47654E+00	0.71244E+00	-0.56067E+00	0.37127E+00	0.34546E-01	0.30716E+00
0.8	0.38195E+00	0.85466E+00	-0.71897E+00	0.45854E+00	0.27053E-01	0.15604E+00
0.9	0.29517E+00	0.10027E+01	-0.88157E+00	0.55939E+00	0.21498E-01	0.83195E-01
1.0	0.21621E+00	0.11550E+01	-0.10467E+01	0.67469E+00	0.17325E-01	0.46670E-01
1.2	0.79739E-01	0.14681E+01	-0.13809E+01	0.95201E+00	0.11690E-01	0.16865E-01
1.4	-0.32479E-01	0.17879E+01	-0.17167E+01	0.12970E+01	0.82383E-02	0.70882E-02
1.6	-0.12545E+00	0.21112E+01	-0.20521E+01	0.17161E+01	0.60167E-02	0.33457E-02
1.8	-0.20326E+00	0.24362E+01	-0.23865E+01	0.22154E+01	0.45256E-02	0.17279E-02
2.0	-0.26909E+00	0.27617E+01	-0.27194E+01	0.28010E+01	0.34889E-02	0.95820E-03
2.2	-0.32537E+00	0.30874E+01	-0.30510E+01	0.34787E+01	0.27461E-02	0.56285E-03
2.4	-0.37393E+00	0.34129E+01	-0.33813E+01	0.42544E+01	0.22003E-02	0.34666E-03
2.6	-0.41622E+00	0.37380E+01	-0.37102E+01	0.51336E+01	0.17901E-02	0.22214E-03
2.8	-0.45333E+00	0.40626E+01	-0.40381E+01	0.61220E+01	0.14761E-02	0.14722E-03
3.0	-0.48614E+00	0.43867E+01	-0.43649E+01	0.72250E+01	0.12315E-02	0.10042E-03

Table 2:

s	$a_C(s)$	a_C(theory $s << 1$)	a_C(theory $s >> 1$)
0.1	0.95894E-02	0.90864E-02	
0.2	0.33586E-01	0.31986E-01	
0.3	0.65420E-01	0.58529E-01	
0.4	0.10168E+00	0.81452E-01	
0.5	0.14132E+00	0.98999E-01	
0.6	0.18387E+00	0.11167E+00	
0.7	0.22894E+00		
0.8	0.27622E+00		
0.9	0.32543E+00		
1.0	0.37634E+00		0.26795E+00
1.2	0.48248E+00		0.35609E+00
1.4	0.59335E+00		0.45064E+00
1.6	0.70806E+00		0.55601E+00
1.8	0.82593E+00		0.65524E+00
2.0	0.94652E+00		0.76393E+00
2.2	0.10695E+01		0.87621E+00
2.4	0.11946E+01		0.99168E+00
2.6	0.13218E+01		0.11100E+01
2.8	0.14509E+01		0.12310E+01
3.0	0.15820E+01		0.13542E+01
3.5	0.19179E+01		0.16716E+01
4.0	0.22661E+01		0.20000E+01
4.5	0.26265E+01		0.23377E+01
5.0	0.29985E+01		0.26834E+01
5.5	0.33799E+01		0.30359E+01
6.0	0.37675E+01		0.33944E+01
7.0	0.45461E+01		0.41270E+01
8.0	0.53124E+01		0.48769E+01
9.0	0.60592E+01		0.56411E+01
10.0	0.67876E+01		0.64174E+01

Table 3:

a	$\hat{\Gamma}_\ell(s,a)$	$\hat{\Gamma}(s,a)$	$\hat{\Gamma}_u(s,a)$	$\hat{R}(s,a)$
0.00	0.23368E+00	0.58440E-01	0.23368E+00	0.12704E+01
0.01	0.25330E+00	0.49498E-01	0.21654E+00	0.13458E+01
0.02	0.27604E+00	0.41336E-01	0.20146E+00	0.14292E+01
0.03	0.30291E+00	0.33948E-01	0.18797E+00	0.15210E+01
0.04	0.33533E+00	0.27330E-01	0.17579E+00	0.16221E+01
0.05	0.37502E+00	0.21475E-01	0.16484E+00	0.17320E+01
0.06	0.42552E+00	0.16374E-01	0.15471E+00	0.18520E+01
0.07	0.49184E+00	0.12014E-01	0.14535E+00	0.19826E+01
0.08	0.58256E+00	0.83815E-02	0.13670E+00	0.21230E+01
0.09	0.71415E+00	0.54554E-02	0.12865E+00	0.22734E+01
0.10	0.92130E+00	0.32090E-02	0.12114E+00	0.24338E+01
0.11	0.12900E+01	0.16064E-02	0.11404E+00	0.26046E+01
0.12	0.21010E+01	0.59730E-03	0.10733E+00	0.27855E+01
0.13	0.49730E+01	0.10605E-03	0.10098E+00	0.29770E+01

Table 4:

a	$\hat{\Gamma}_\ell(s,a)$	$\hat{\Gamma}(s,a)$	$\hat{\Gamma}_u(s,a)$	$\hat{R}(s,a)$
0.00	0.67470E+00	0.17325E-01	0.67470E+00	0.46670E-01
0.02	0.71296E+00	0.15210E-01	0.63843E+00	0.50861E-01
0.04	0.75373E+00	0.13258E-01	0.60382E+00	0.55615E-01
0.06	0.79762E+00	0.11462E-01	0.57062E+00	0.61686E-01
0.08	0.84558E+00	0.98168E-02	0.53863E+00	0.69172E-01
0.10	0.89872E+00	0.83175E-02	0.50779E+00	0.78431E-01
0.12	0.95870E+00	0.69593E-02	0.47797E+00	0.89926E-01
0.14	0.10276E+01	0.57375E-02	0.44922E+00	0.10426E+00
0.16	0.11086E+01	0.46478E-02	0.42147E+00	0.12222E+00
0.18	0.12060E+01	0.36860E-02	0.39481E+00	0.14482E+00
0.20	0.13263E+01	0.28481E-02	0.36920E+00	0.17341E+00
0.22	0.14798E+01	0.21299E-02	0.34470E+00	0.20969E+00
0.24	0.16830E+01	0.15271E-02	0.32132E+00	0.25587E+00
0.26	0.19653E+01	0.10350E-02	0.29908E+00	0.31471E+00
0.28	0.23833E+01	0.64842E-03	0.27799E+00	0.38961E+00
0.30	0.30613E+01	0.36111E-03	0.25806E+00	0.48459E+00
0.32	0.43304E+01	0.16548E-03	0.23926E+00	0.60420E+00
0.34	0.74259E+01	0.51541E-04	0.22159E+00	0.75330E+00
0.36	0.22781E+02	0.50140E-05	0.20503E+00	0.93697E+00
0.37	0.14943E+03	0.11033E-06	0.19715E+00	0.10435E+01

Table 5:

$s = 0.5$			$s = 1.0$		
a	$W_\ell \hat{f}_\ell(s,a)$	$W_u \hat{f}_u(s,a)$	a	$W_\ell \hat{f}_\ell(s,a)$	$W_u \hat{f}_u(s,a)$
0.00	0.22532E+00	0.22532E+00	0.00	0.57047E+00	0.57047E+00
0.01	0.24279E+00	0.20983E+00	0.02	0.59332E+00	0.54781E+00
0.02	0.26269E+00	0.19598E+00	0.04	0.61648E+00	0.52524E+00
0.03	0.28567E+00	0.18347E+00	0.06	0.64013E+00	0.50272E+00
0.04	0.31257E+00	0.17209E+00	0.08	0.66448E+00	0.48022E+00
0.05	0.34445E+00	0.16169E+00	0.10	0.68980E+00	0.45777E+00
0.06	0.38296E+00	0.15208E+00	0.12	0.71639E+00	0.43541E+00
0.07	0.43030E+00	0.14317E+00	0.14	0.74462E+00	0.41320E+00
0.08	0.48957E+00	0.13489E+00	0.16	0.77489E+00	0.39121E+00
0.09	0.56528E+00	0.12715E+00	0.18	0.80764E+00	0.36956E+00
0.10	0.66386E+00	0.11990E+00	0.20	0.84340E+00	0.34832E+00
0.11	0.79418E+00	0.11306E+00	0.22	0.88267E+00	0.32760E+00
0.12	0.96684E+00	0.10661E+00	0.24	0.92597E+00	0.30748E+00
0.13	0.11881E+01	0.10050E+00	0.26	0.97375E+00	0.28805E+00
			0.28	0.10263E+01	0.26937E+00
			0.30	0.10834E+01	0.25150E+00
			0.32	0.11441E+01	0.23448E+00
			0.34	0.12055E+01	0.21832E+00
			0.36	0.12614E+01	0.20304E+00

Figure 1:

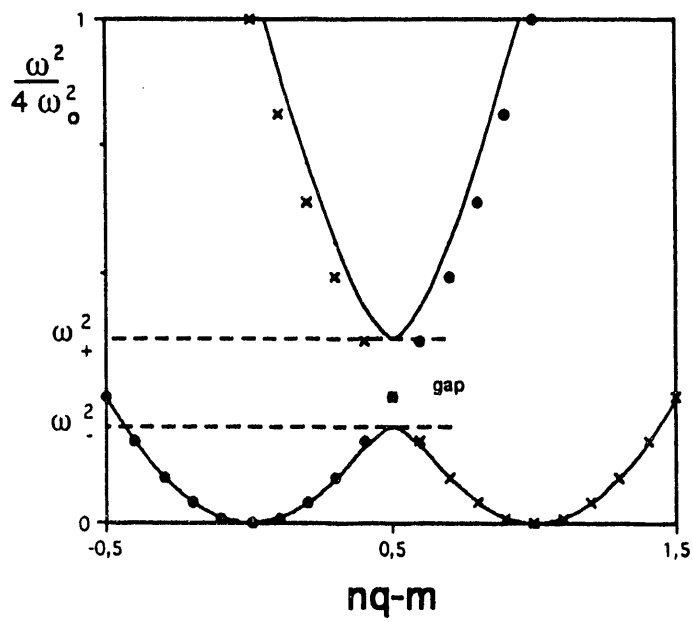

Figure 2:

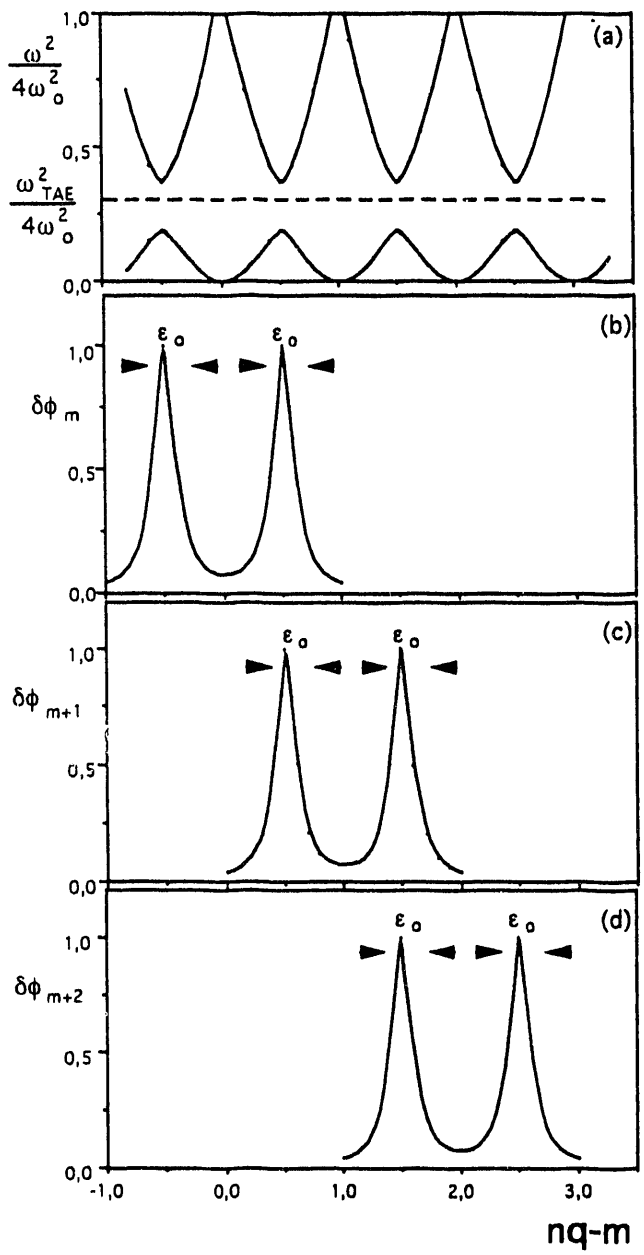
(a)
1,0
0,5
0,0
$\frac{\omega^2}{4\omega_o^2}$
$\frac{\omega^2_{TAE}}{4\omega_o^2}$
(b)
ε_o
ε_o
$\delta\phi_m$
(c)
$\delta\phi_{m+1}$
(d)
$\delta\phi_{m+2}$
-1,0
0,0
1,0
2,0
3,0
nq-m

Figure 3:

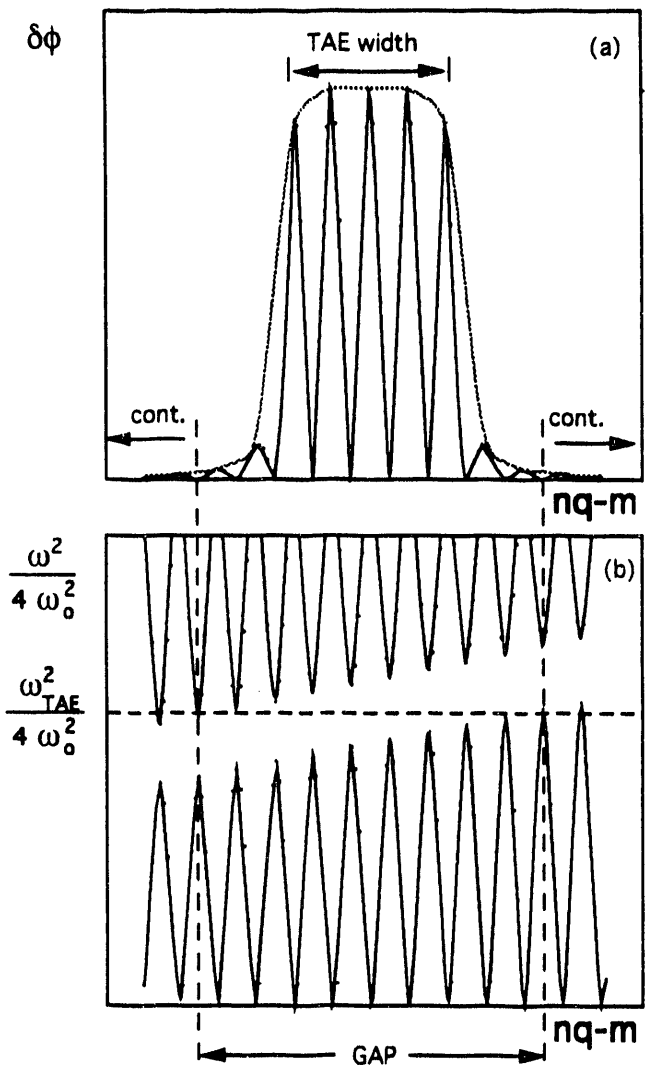

Figure 4:

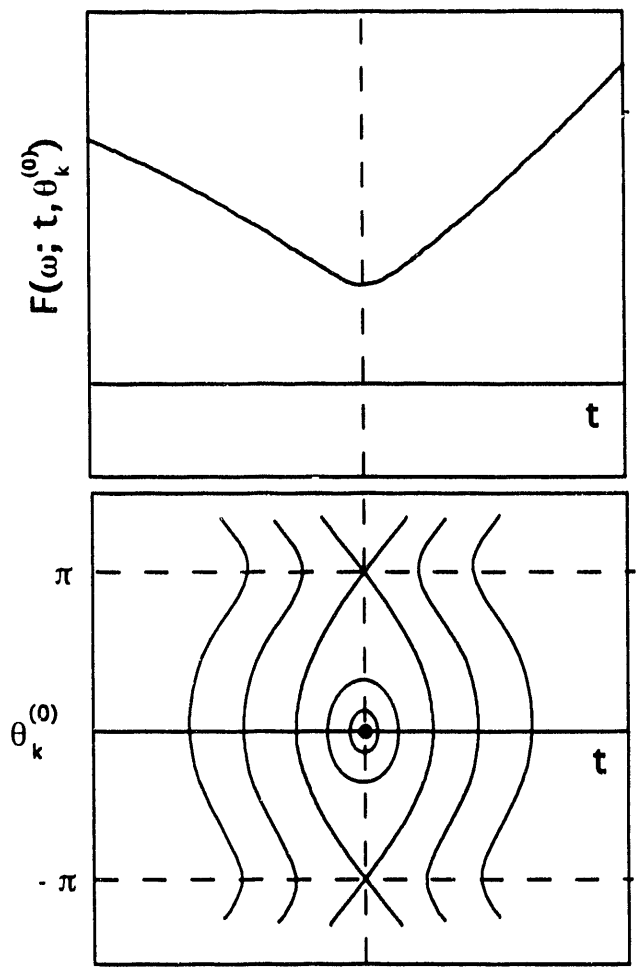

Figure 5:

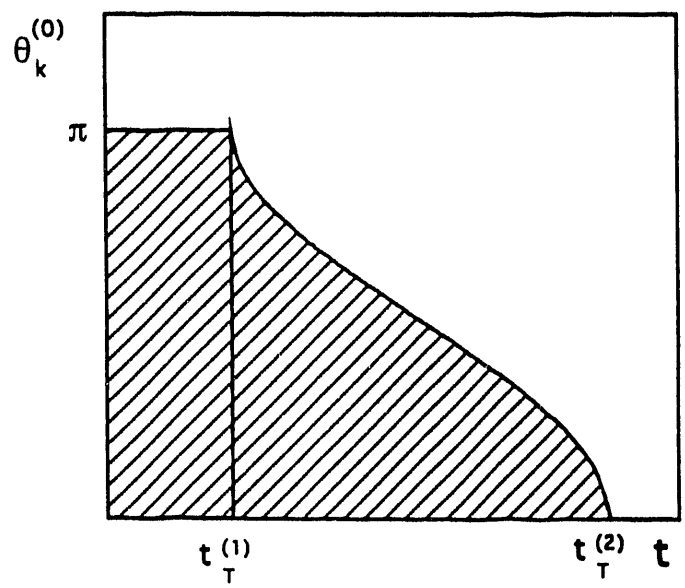

EXTERNAL DISTRIBUTION IN ADDITION TO UC-420

Dr. F. Paoloni, Univ. of Wollongong, AUSTRALIA
Prof. M.H. Brennan, Univ. of Sydney, AUSTRALIA
Plasma Research Lab., Australian Nat. Univ., AUSTRALIA
Prof. I.R. Jones, Flinders Univ, AUSTRALIA
Prof. F. Cap, Inst. for Theoretical Physics, AUSTRIA
Prof. M. Heindler, Institut für Theoretische Physik, AUSTRIA
Prof. M. Goossens, Astronomisch Instituut, BELGIUM
Ecole Royale Militaire, Lab. de Phy. Plasmas, BELGIUM
Commission-European, DG. XII-Fusion Prog., BELGIUM
Prof. R. Boucique, Rijksuniversiteit Gent, BELGIUM
Dr. P.H. Sakanaka, Instituto Fisica, BRAZIL
Instituto Nacional De Pesquisas Espaciais-INPE, BRAZIL
Documents Office, Atomic Energy of Canada Ltd., CANADA
Dr. M.P. Bachynski, MPB Technologies, Inc., CANADA
Dr. H.M. Skarsgard, Univ. of Saskatchewan, CANADA
Prof. J. Teichmann, Univ. of Montreal, CANADA
Prof. S.R. Sreenivasan, Univ. of Calgary, CANADA
Prof. T.W. Johnston, INRS-Energie, CANADA
Dr. R. Bolton, Centre canadien de fusion magnétique, CANADA
Dr. C.R. James,, Univ. of Alberta, CANADA
Dr. P. Lukác, Komenského Universzita, CZECHO-SLOVAKIA
The Librarian, Culham Laboratory, ENGLAND
Library, R61, Rutherford Appleton Laboratory, ENGLAND
Mrs. S.A. Hutchinson, JET Library, ENGLAND
Dr. S.C. Sharma, Univ. of South Pacific, FIJI ISLANDS
P. Mähönen, Univ. of Helsinki, FINLAND
Prof. M.N. Bussac, Ecole Polytechnique,, FRANCE
C. Mouttet, Lab. de Physique des Milieux Ionisés, FRANCE
J. Radet, CEN/CADARACHE - Bat 506, FRANCE
Prof. E. Economou, Univ. of Crete, GREECE
Ms. C. Rinni, Univ. of Ioannina, GREECE
Dr. T. Mual, Academy Bibliographic Ser., HONG KONG
Preprint Library, Hungarian Academy of Sci., HUNGARY
Dr. B. DasGupta, Saha Inst. of Nuclear Physics, INDIA
Dr. P. Kaw, Inst. for Plasma Research, INDIA
Dr. P. Rosenau, Israel Inst. of Technology, ISRAEL
Librarian, International Center for Theo Physics, ITALY
Miss C. De Palo, Associazione EURATOM-ENEA , ITALY
Dr. G. Grosso, Istituto di Fisica del Plasma, ITALY
Prof. G. Rostangni, Istituto Gas Ionizzati Del Cnr, ITALY
Dr. H. Yamato, Toshiba Res & Devel Center, JAPAN
Prof. I. Kawakami, Hiroshima Univ., JAPAN
Prof. K. Nishikawa, Hiroshima Univ., JAPAN
Director, Japan Atomic Energy Research Inst., JAPAN
Prof. S. Itoh, Kyushu Univ., JAPAN
Research Info. Ctr., National Instit. for Fusion Science, JAPAN
Prof. S. Tanaka, Kyoto Univ., JAPAN
Library, Kyoto Univ., JAPAN
Prof. N. Inoue, Univ. of Tokyo, JAPAN
Secretary, Plasma Section, Electrotechnical Lab., JAPAN
S. Mori, Technical Advisor, JAERI, JAPAN
Dr. O. Mitarai, Kumamoto Inst. of Technology, JAPAN
J. Hyeon-Sook, Korea Atomic Energy Research Inst., KOREA
D.I. Choi, The Korea Adv. Inst. of Sci. & Tech., KOREA
Prof. B.S. Liley, Univ. of Waikato, NEW ZEALAND
Inst of Physics, Chinese Acad Sci PEOPLE'S REP. OF CHINA
Library, Inst. of Plasma Physics, PEOPLE'S REP. OF CHINA
Tsinghua Univ. Library, PEOPLE'S REPUBLIC OF CHINA
Z. Li, S.W. Inst Physics, PEOPLE'S REPUBLIC OF CHINA
Prof. J.A.C. Cabral, Instituto Superior Tecnico, PORTUGAL
Dr. O. Petrus, AL I CUZA Univ., ROMANIA
Dr. J. de Villiers, Fusion Studies, AEC, S. AFRICA
Prof. M.A. Hellberg, Univ. of Natal, S. AFRICA
Prof. D.E. Kim, Pohang Inst. of Sci. & Tech., SO. KOREA
Prof. C.I.E.M.A.T, Fusion Division Library, SPAIN
Dr. L. Stenflo, Univ. of UMEA, SWEDEN
Library, Royal Inst. of Technology, SWEDEN
Prof. H. Wilhelmson, Chalmers Univ. of Tech., SWEDEN
Centre Phys. Des Plasmas, Ecole Polytech, SWITZERLAND
Bibliotheek, Inst. Voor Plasma-Fysica, THE NETHERLANDS
Asst. Prof. Dr. S. Cakir, Middle East Tech. Univ., TURKEY
Dr. V.A. Glukhikh,Sci. Res. Inst. Electrophys.I Apparatus, USSR
Dr. D.D. Ryutov, Siberian Branch of Academy of Sci., USSR
Dr. G.A. Eliseev, I.V. Kurchatov Inst., USSR
Librarian, The Ukr.SSR Academy of Sciences, USSR
Dr. L.M. Kovrizhnykh, Inst. of General Physics, USSR
Kernforschungsanlage GmbH, Zentralbibliothek, W. GERMANY
Bibliothek, Inst. Für Plasmaforschung, W. GERMANY
Prof. K. Schindler, Ruhr-Universität Bochum, W. GERMANY
Dr. F. Wagner, (ASDEX), Max-Planck-Institut, W. GERMANY
Librarian, Max-Planck-Institut, W. GERMANY
Prof. R.K. Janev, Inst. of Physics, YUGOSLAVIA

END

DATE
FILMED
8/27/93